in product analysis after photolysis under continuous irradiation. The slope of the Hammett plot of log k vs σ_p is equal to +1.0; the positive value of σ is consistent with the electrophilic addition of the benzaldehyde to the carbonyl ylide. Theoretically, the decay of ylide 3a must be equal to the growth of dioxole 5a if HCl elimination is rapid. Attempts have been made to follow the growth of 5a. However, no transient spectrum was observed at 440 nm during the few milliseconds following the excitation. On the other hand, the failure to isolate dioxolane 4a under medium-pressure liquid chromatography on silica gel suggests that the elimination of HCl from 4a occurs within a few minutes at room temperature.

In the absence of acetone, the laser photolysis of 1a in isooctane in the presence of benzaldehyde produced a new transient absorption ($\lambda_{max} = 530$ nm). This transient absorption is assigned to the carbonyl ylide 11 formed by reaction of carbene 2a with benzaldehyde. Measurement of the rate of growth of the ab-

sorption at 530 nm as a function of [benzaldehyde] yielded the rate constant for ylide formation, $k = 1.1 \times 10^9$ M^{-1} s^{-1}. The ylide 11 is subsequently quenched by benzaldehyde, as shown by the dependence of its decay time on [benzaldehyde] but, since this decay does not fit a first-order law, the quenching rate constant is not easily extracted from the kinetic data. Thus, benzaldehyde plays a double role, first as a constituent of a carbonyl ylide and then as a dipolarophile in the trapping of the ylide. Huisgen and de March[11] reported a similar mechanism to explain the formation of the diastereoisomeric 1,3-dioxolanes and oxirane in the thermal reaction of dimethyl diazomalonate with an excess of benzaldehyde.

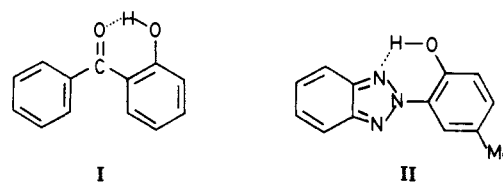# Photoinduced Intramolecular Proton Transfer as the Mechanism of Ultraviolet Stabilizers: A Reappraisal

Javier Catalán,*,† Fernando Fabero,† M. Soledad Guijarro,† Rosa M. Claramunt,*,‡ M. Dolores Santa María,‡ M. de la Concepción Foces-Foces,§ Felix Hernández Cano,§ José Elguero,⊥ and Roberto Sastre‖

Contribution from the Departamento de Química, Física, Facultad de Ciencias, Universidad Autónoma de Madrid, Cantoblanco, 28049 Madrid, Spain, Departamento de Química Orgánica, UNED, 28040 Madrid, Spain, U.E.I. de Cristalografía, Instituto de Química Física "Rocasolano", CSIC, 28006 Madrid, Spain, Instituto de Química Médica, CSIC, 28006 Madrid, Spain, and Instituto de Ciencia y Tecnología de Polímeros, CSIC, 28006 Madrid, Spain. Received June 29, 1989

Abstract: Evidence based on theoretical calculations and photophysical experiments is presented to show that, contrary to general belief, the photostability of 2-(2'-hydroxy-5'-methylphenyl)benzotriazole (Tinuvin P) cannot be explained as being due to an excited-state intramolecular proton transfer (ESIPT) through the intramolecular hydrogen bond (IMHB). Support for this conclusion comes from a related study on several members of a new family of photostable compounds, namely the 1-(2'-hydroxyphenyl)pyrazoles, which were obtained by the reaction of pyrazole and of 3,5-dimethylpyrazole with benzoquinone. The structures of these pyrazole derivatives, namely 2,3-bis(3',5'-dimethylpyrazol-1'-yl)-, 2,3-bis(pyrazol-1'-yl)-, 2-(pyrazol-1'-yl)-, and 2,5-bis(pyrazol-1'-yl)-1,4-dihydroxybenzene (1, 2, 3, and 4, respectively) were established by spectroscopic techniques and X-ray crystallography. Both derivatives 3 and 4 possess a strong intramolecular hydrogen bond and are reasonably photostable; derivatives 1 and 2 appear, however, to possess only a weak intramolecular hydrogen bond. 1 and 3 pack in helical systems, 4 does it with intercrossing stacking, and 2·H$_2$O has a three-dimensional network involving water molecules.

An important class of photostabilizers are the ultraviolet absorbers or light screeners; these colorless or nearly colorless organic compounds are able to protect polymers and other light-sensitive materials from degradation caused by the ultraviolet component of sunlight and various kinds of artificial light. In the chemical structure of such compounds, it is usual[1] to find a phenolic group which is intramolecularly hydrogen bonded (IMHB) to a heteroatom as oxygen or nitrogen of the same chromophore. Important families of such photostabilizers are the 2-hydroxybenzophenones (represented by the parent compound (I)) and the 2-(2'-hydroxyphenyl)benzotriazoles (represented by the methyl derivative (II) commonly known as Tinuvin P).

In order to explain the large Stokes shift (11 000 cm^{-1}) observed in the fluorescence spectrum of methyl salicylate (III), Weller[2]

I   II

proposed the so-called ESIPT (excited-state intramolecular proton transfer) model (IIIb → IIIc), with proton transfer taking place along the IMHB.

This model has led some authors[1,3-7] to suggest that the photostability of such compounds is due to a rapid nonradiative deactivation of the quinonoid form IIIc, due to the dramatic approximation of the electronic states implicated in the intramolecular proton transfer. This process regenerates the original form IIIa and confers upon methyl salicylate a high stability to ultraviolet light.

* Authors to whom correspondence should be addressed.
† Departamento de Química, UAM.
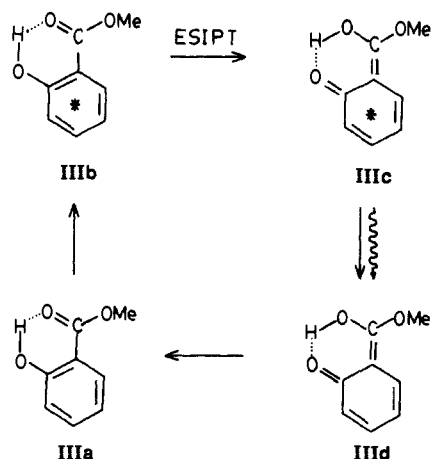‡ Departamento de Química Orgánica, UNED.
§ Instituto Rocasolano, CSIC.
⊥ Instituto de Química Médica, CSIC.
‖ Instituto de Ciencia y Tecnología de Polímeros, CSIC.

(1) Heller, H. J. *Eur. Polym. J. Suppl.* 1969, 105.

748 *J. Am. Chem. Soc., Vol. 112, No. 2, 1990*

Catalan et al.

Scheme I

Although this mechanism is still accepted and has been the subject of a large number of papers on related structures,[2-68] a careful analysis of the literature shows that it may not be valid.

For example, the conclusion that in the deactivation of the quinonoid form generated via ESIPT (IIIc → IIId) the nonra-
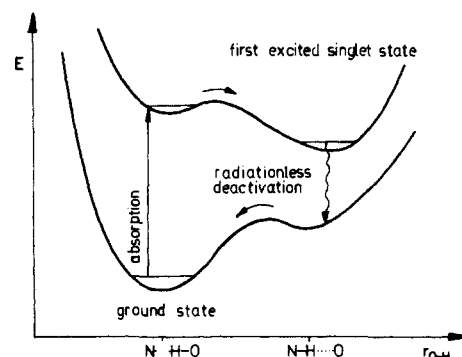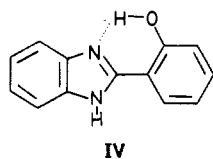

Figure 1. Deactivation scheme proposed by Otterstedt.[5]

diative process is the most efficient one was deduced from the fact that, in general, these compounds do not show fluorescence in nonpolar solvents at room temperature. However, it has been established that some compounds, e.g., the 2-(2'-hydroxy-phenyl)benzimidazoles[59] (HPBI, IV) are converted by light into a quinonoid form via the ESIPT mechanism (Figure 1) with such a high fluorescence quantum yield that they behave as efficient laser dyes by intramolecular proton transfer.[69,70]

(2) Weller, A. *Naturwissenshaften* **1955**, *42*, 175; *Z. Elektrochem.* **1956**, *60*, 1144.

(3) Williams, D. L.; Heller, A. *J. Phys. Chem.* **1970**, *74*, 4473.

(4) Heller, H. J.; Blattman, H. R. *Pure Appl. Chem.* **1972**, *30*, 145 and **1973**, *36*, 141.

(5) Otterstedt, J. E. A. *J. Phys. Chem.* **1973**, *58*, 5716.

(6) Klöpffer, W. In *Advances in Photochemistry*; Pitts, J. N., Jr., Hammond, S. S., Gollnick, K., Eds.; Wiley: New York, 1977; Vol 10; p 311 and references therein.

(7) Werner, T. *J. Phys. Chem.* **1979**, *83*, 320.

(8) Marsh, J. K. *J. Chem. Soc.* **1924**, *125*, 418.

(9) Lamola, A. A.; Sharp, L. J. *J. Phys. Chem.* **1966**, *70*, 2634.

(10) Klöpffer, W.; Naudorf, G. *J. Lumin.* **1974**, *11*, 249.

(11) Catalan, J.; Fernández-Alonso, J. I. *J. Mol. Struct.* **1975**, *27*, 303.

(12) Kosower, E. M.; Dodiuk, H. *J. Lumin*, **1975/76**, *11*, 249.

(13) Sandros, K. *Acta Chem. Scand. Ser. A* **1976**, *30*, 761.

(14) Catalan, J.; Tomas, F. *Adv. Mol Relaxation Processes.* **1976**, *8*, 87.

(15) Shizuka, H.; Matsui, K.; Tanaka, I. *J. Phys. Chem.* **1977**, *81*, 2243.

(16) Nakagaki, R.; Kobayashi, T.; Nagakura, S. *Bull. Chem. Soc. Jpn.* **1978**, *51*, 1671.

(17) Goodman, J.; Brus, L. E. *J. Am. Chem. Soc.* **1978**, *100*, 7422.

(18) Smith, K. K.; Kaufmann, G. *J. Phys. Chem.* **1978**, *82*, 2286.

(19) Klopffer, W.; Kaufmann, G. *J. Lumin.* **1979**, *20*, 283.

(20) Hou, S.-Y.; Hetherington, III, W. M.; Korenowski, G. M.; Eisenthal, K. B. *Chem. Phys. Lett.* **1979**, *68*, 282.

(21) Rossetti, R.; Brus, L. E. *J. Chem. Phys.* **1980**, *73*, 1547.

(22) Rossetti, R.; Haddon, R. C.; Brus, L. E. *J. Am. Chem. Soc.* **1980**, *102*, 6913.

(23) Ford, D.; Thistlethwaite, P. J.; Woolfe, G. J. *Chem. Phys. Lett.* **1980**, *69*, 246.

(24) Acuña, A.; Amat-Guerri, F.; Catalan, J.; Gonzalez-Tablas, F. *J. Phys. Chem.* **1980**, *84*, 629.

(25) Merritt, C.; Scott, G. W.; Gupta, A.; Yavrouian, A. *Chem. Phys. Lett.* **1980**, *69*, 169.

(26) Heimbrok, L. A.; Kenny, J. E.; Kohler, B. E.; Scott, G. W. *J. Chem. Phys.* **1981**, *75*, 5201.

(27) Acuña, A. U.; Catalan, J.; Toribio, F. *J. Phys. Chem.* **1981**, *85*, 241.

(28) Lopez-Delgado, R.; Lazare, S. *J. Phys. Chem.* **1981**, *85*, 763.

(29) Smith, K. K.; Kaufmann, K. J. *J. Phys. Chem.* **1981**, *85*, 2895.

(30) Rossetti, R.; Rayford, R.; Haddon, R. C.; Brus, L. E. *J. Am. Chem. Soc.* **1981**, *103*, 4303.

(31) Woolfe. G. J.; Thislethwaite, P. J. *J. Am. Chem. Soc.* **1981**, *103*, 3849.

(32) Mordzinski, A.; Grabowska, A. *Chem. Phys. Lett.* **1983**, *90*, 122.

(33) Catalan, J.; Toribio, F.; Acuña, A. *J. Phys. Chem.* **1982**, *86*, 303.

(34) Huston, A. L.; Scott, G. W.; Gupta, A. *J. Chem. Phys.* **1982**, *76*, 4978.

(35) Flom, S. R.; Barbara, P. F. *Chem. Phys. Lett.* **1983**, *94*, 488.

(36) Bocian, D. F.; Huston, A. L.; Scott, G. W. *J. Chem. Phys.* **1983**, *79*, 5802.

(37) Ding, K.; Courtney, S. J.; Strandjord, A. J.; Flom, S.; Friedrich, D.; Barbara, P. F. *J. Phys. Chem.* **1983**, *87*, 1184.

(38) Heimbrook, L. A.; Kenny, J. E.; Kohler, B. E.; Scott, G. W. *J. Phys. Chem.* **1983**, *87*, 280.

(39) Toribio, F.; Catalan, J.; Amat-Guerri, F.; Acuña, A. U. *J. Phys. Chem.* **1983**, *87*, 817.

(40) Mordzinski, A.; Grabowska, A.; Kühnle, W.; Krowczynski, A. *Chem. Phys. Lett.* **1983**, *101*, 291.

(41) Brackmann, U.; Ernsting, N. P.; Ouw, D.; Schmitt, K. *Chem. Phys. Lett.* **1984**, *110*, 319.

(42) Mordzinski, A.; Grabowska, A.; Teuchner, K. *Chem. Phys. Lett.* **1984**, *111*, 383.

(43) Mordzinski, A.; Grabowska, A. *J. Mol. Struct.* **1984**, *114*, 337.

(44) Wössner, G.; Goeller, G.; Kollat, P.; Stozowski, J. J.; Hauser, M.; Klein, U. K. A.; Kramer, H. E. A. *J. Phys. Chem.* **1984**, *88*, 5544.

(45) O'Connor, D. B.; Scott, G. W.; Coulter, D. R.; Gupta, A.; Webb, S. P.; Yeh, S. W.; Clark, J. H. *Chem. Phys. Lett.* **1985**, *121*, 417.

(46) Acuña, A. U.; Toribio, F.; Amat-Guerri, F.; Catalan, J. *J. Photochem.* **1985**, *30*, 339.

(47) Sanchez-Cabezudo, M.; De Paz, J. L. G.; Catalan, J.; Amat-Guerri, F. *J. Mol. Struct.* **1985**, *131*, 277.

(48) Ernsting, N. P. *J. Phys. Chem.* **1985**, *89*, 4932.

(49) Jang, D. J.; Kelley, D. F. *J. Phys. Chem.* **1985**, *89*, 209.

(50) Shizuka, H.; Machii, M.; Higaki, Y.; Tanaka, M.; Tanaka, I. *J. Phys. Chem.* **1985**, *89*, 320.

(51) Wössner, G.; Goeller, G.; Rieke, J.; Hoier, H.; Stezowski, J. J.; Daltrozzo, E.; Neurieter, M.; Kramer, H. E. A. *J. Phys. Chem.* **1985**, *89*, 3629.

(52) Itoh, M.; Fujiwara, Y. *J. Am. Chem. Soc.* **1985**, *107*, 1561.

(53) Jang, D. J.; Brucker, G. A.; Kelley, D. F. *J. Phys. Chem.* **1986**, *90*, 6808.

(54) Elsaesser, T.; Kaiser, W.; Lütke, W. *J. Phys. Chem.* **1986**, *90*, 2901.

(55) Gillispie, G. D.; Van Benthem, M. N.; Vangsness, M. *J. Phys. Chem.* **1986**, *90*, 2596 and references therein.

(56) Mordzinski, A.; Kühnle, W. *J. Phys. Chem.* **1986**, *90*, 1455.

(57) Nishiya, T.; Yamauchi, S.; Hirota, N.; Fujiwara, Y.; Itoh, M. *J. Am. Chem. Soc.* **1986**, *108*. 3880.

(58) Nishiya, T.; Yamauchi, S.; Hirota, N.; Baba, M.; Hanazaki, J. *J. Phys. Chem.* **1986**, *90*, 5730.

(59) Sinha, H. K.; Dogra, S. K. *Chem. Phys.* **1986**, *102*, 337.

(60) Ghiggino, K. P.; Scully, A. D.; Leaver, I. H. *J. Phys. Chem.* **1986**, *90*, 5089.

(61) Mordzinski, A.; Grellmann, K. H. *J. Phys. Chem.* **1986**, *90*, 5503.

(62) Waluk, J.; Bulska, H.; Grabowsa, A.; Mordzinski, A. *New J. Chem.* **1986**, *10*, 413.

(63) Ernsting, N. P.; Mordzinski, A.; Dick, B. *J. Phys. Chem.* **1987**, *91*, 1404.

(64) Huston, A. L.; Scott, G. W. *J. Phys. Chem.* **1987**, *91*, 1408.

(65) Becker, R. S.; Lenoble, C.; Zein, A. *J. Phys. Chem.* **1987**, *91*, 3509 and 3517.

(66) Rodriguez-Prieto, M. F.; Nickel, B.; Grellmann, K. H.; Mordzinski, A. *Chem. Phys. Lett.* **1988**, *146*, 387.

(67) Yamauchi, S.; Hirota, N. *J. Am. Chem. Soc.* **1988**, *110*, 1346.

(68) Goeller, G.; Riecker, J.; Maier, A.; Sterowski, J. J.; Daltrozzo, E.; Neurieter, M.; Port, H.; Wiechmann, M.; Kramer, E. A. *J. Phys. Chem.* **1988**, *92*, 1452.

Photoinduced Intramolecular Proton Transfer

J. Am. Chem. Soc., Vol. 112, No. 2, 1990 749

IV

Furthermore, it cannot be said that our understanding of the photophysical properties of Tinuvin P (TIN, 2-(2'-hydroxy-5'-methylphenyl)benzotriazole, II) about which all of our knowledge on this field has been accumulated (cf., the pioneer work of Heller[1]) is complete. For example, we do not know if Tinuvin P exists in nonpolar solvents as a unique structure or as a mixture of planar and nonplanar forms, nor do we know its structure in solvents with which it can form hydrogen bonds, or why the emission of the quinonoid form generated via an ESIPT mechanism has not been detected at room temperature. *In other words,* which molecular conformation (or conformations) of Tinuvin P is responsible for its photostability?

It is relevant to notice that very recently Rabek[71] pointed out that "It is doubtful whether the intramolecular proton-transfer cycle alone can be responsible for the photostabilization of polymers by (o-hydroxyphenyl)benzotriazoles", and even Goeller et al.[68] were compelled to introduce modifications to the IMHB–ESIPT model to explain why for crystalline TIN the effect of temperature is more important on the fluorescence quantum yields than on the lifetimes.

Due to the commercial importance[72] of the (o-hydroxyphenyl)benzotriazole class of UV stabilizers, several attempts to prepare new photostable compounds by changing the azole counterpart have been described in the literature:[1,71-74] The 2-(2'-hydroxyphenyl)benzoxazoles, 2-(2'-hydroxyphenyl)benzothiazoles, 2-(2'-hydroxyphenyl)benzimidazoles, IV, 3-(2'-hydroxyphenyl)-1,2,4-triazoles, and 2-(2'-hydroxyphenyl)-1,3,4-triazoles have been investigated, but all have failed to show useful photoprotector properties.

The aim of the present work was (i) to prepare new heterocyclic compounds based on pyrazole which contain a phenolic hydroxyl group capable of forming an IMHB with one of the pyrazole nitrogen atoms and (ii) to determine their photostabilities in the hope of being able to shed light on the mechanism of the photostability of such compounds in general.

Experimental Section

General Methods. Melting points were recorded in a capillary tube on a Büchi 530 apparatus and are uncorrected. Mass spectra were obtained on a VG-12-250 spectrometer at 70 eV. Nuclear magnetic resonance spectra were obtained on a Bruker AC-200 with standard conditions. Chemical shifts (δ) in ppm and coupling constants (J) in Hz were measured in deuteriochloroform or hexadeuteriodimethyl sulfoxide referred to TMS as internal standard. The ^{1}H and ^{13}C chemical shifts are accurate to 0.01 and 0.1 ppm, respectively. Coupling constants are accurate to ± 0.2 Hz for ^{1}H NMR and ± 0.6 Hz for the ^{13}C NMR. The data acquisition parameters for the heteronuclear (^{1}H–^{13}C) 2D correlation experiments were F_1 domain (SI1, 256 W; SW1, 1099 Hz; relaxation delay D1, 1s), F_2 domain (SI2, 4K; SW2, 10000 Hz), number of transients per FID, NS, 128; number of preparatory dummy transients per FID, DS, O and J values of 166, 10, 7, and 3 Hz. All the 2D experiments were processed with a sine bell window (WDW1 = WDW2 = S, SSB1 = 0, SSB2 = 2). Analytical thin layer chromatography was performed on silica gel Merck Kiesegel 60 F$_{254}$ with a layer thickness of 0.2 mm. Column chromatography with silica gel Merck 60 (70–230 mesh,

(69) Acuña, A. U.; Amat-Guerri, F.; Catalan, J.; Costela, A.; Figuera, J. M.; Muñoz, J. M. *Chem. Phys. Lett.* **1986**, *132*, 567.

(70) Costela, A.; Amat-Guerri, F.; Catalan, J.; Douhal, A.; Figuera, J. M.; Muñoz, J. M.; Acuña, A. U. *Opt. Commun.* **1987**, *64*, 457.

(71) Rabek, J. F. In *Mechanisms of Photophysical Processes and Photochemical Reactions in Polymers*; Wiley: New York, 1987.

(72) Dexter, M. In *Encyclopedia of Polymers Science and Technology*; Interscience Publishers: New York, 1980; Vol. 23, p 615.

(73) Scott, G. In *New Trends in the Photochemistry of Polymers*; Allen, N. S., Rabek. J. F., Eds.; Elsevier Applied Science Publishers: Londres, 1985; Chapter 14.

(74) Gupta, A.; Liang, R. H.; Vogl, O.; Pradellock, W.; Huston, A. L.; Scott, G. W. In *Physicochemical Aspects of Polymer Surfaces*; Mittal. K. L., Ed.; Plenum Press: New York; 1983; Vol. 1, pp 293–303.

Syntheses. 1,4-Dihydroxy-2,3-bis(3',5'-dimethylpyrazol-1'-yl)benzene (1) and 1,4-Dihydroxy-2-(3',5'-dimethylpyrazol-1'-yl)benzene (5). A mixture of 3,5-dimethylpyrazole (2.5 g, 0.027 mol) and p-benzoquinone (2.8 g, 0.026 mol) in dry dioxane (15 mL) was heated under reflux for 1 h. After cooling, the solvent was removed under reduced pressure, and the crude product was chromatographed on a silica gel column with hexane–ethyl ether (3:7) as eluent to give: 1,4-dihydroxybenzene (R_f 0.31), 1,4-dihydroxy-2-(3',5'-dimethylpyrazol-1'-yl)benzene (5) (R_f 0.21), [mp 232–3 °C, 10% yield, mass spectrum (m/z) 204 (100, M^{*+}). Anal. Calcd for $C_{11}H_{12}N_2O_2$: C, 64.69; H, 5.92; N, 13.72. Found: C, 64.63; H, 6.08; N, 13.49%.], and 1,4-dihydroxy-2,3-bis(3',5'-dimethylpyrazol-1'-yl)benzene (1) (R_f 0.07): mp 281–2 °C, 35% yield, mass spectrum (m/z) 298 (100, M^{*+}). Anal. Calcd for $C_{16}H_{18}N_4O_2$: C, 64.41; H, 6.08; N, 18.78. Found: C, 64.19; H, 6.30; N, 18.62.

1,4-Dihydroxy-2,3-bis(pyrazol-1'-yl)benzene (2), 1,4-Dihydroxy-2-(pyrazol-1'-yl)benzene (3), and 1,4-Dihydroxy-2,5-bis(pyrazol-1'-yl)benzene (4). A mixture of pyrazole (2.5 g, 0.037 mol) and p-benzoquinone (3.97 g, 0.037 mol) in dry dioxane (15 mL) was heated under reflux for 1 h. After cooling, the solvent was removed, and the crude product was chromatographed with chloroform–ethanol (95:5) to give 1,4-dihydroxy-2,5-bis(pyrazol-1'-yl)benzene (4) (R_f 0.61) [mp 206 °C, 10% yield, mass spectrum (m/z) 242 (100, M^{*+}). Anal. Calcd for $C_{12}H_{10}N_4O_2$: C, 59.50; H, 4.16; N, 23.13. Found: C, 59.61; H, 4.16; N, 22.98], and 1,4-dihydroxybenzene (R_f 0.13).

Intermediate fractions with R_f values of 0.30–0.33 in chloroform–ethanol (95:5) contained a mixture of two products, and therefore the residue obtained by removal of the solvent was purified again by column chromatography with hexane–ethyl acetate (6:4) as eluent, to give 1,4-dihydroxy-2-(pyrazol-1'-yl)benzene (3) (R_f 0.24) [mp 181 °C, 30% yield, mass spectrum (m/z) 176 (100, M^{*+}). Anal. Calcd for $C_9H_8N_2O_2$: C, 61.36; H, 4.58; N, 15.90. Found: C, 61.60; H, 4.70; N, 15.63.], and 1,4-dihydroxy-2,3-bis(pyrazol-1'-yl)benzene (2) (R_f 0.13): mp 177 °C, 16% yield, mass spectrum (m/z) 242 (100, M^{*+}). Anal. Calcd for $C_{12}H_{10}N_4O_2$: C, 59.50; H, 4.16; N, 23.13. Found: C, 59.70; H, 4.40; N, 23.24.

Crystal Structure Determinations. 1,4-Dihydroxy-2,3-bis(3',5'-dimethylpyrazol-1'-yl)benzene (1) was crystallized from chloroform–hexane; 1,4-dihydroxy-2,3-bis(pyrazol-1'-yl)benzene (2) and 1,4-dihydroxy-2-bis(pyrazol-1'-yl)benzene (3) from chloroform, and 1,4-dihydroxy-2,5-bis(pyrazol-1'-yl)benzene (4) from chloroform–ethanol.

Crystal Data. (1): $C_{16}H_{18}N_4O_2$, M = 298.34, hexagonal, $P6_122$ ($P6_522$, see below), $a = b = 9.2617$ (2) Å, $c = 32.0236$ (24) Å, $D_c = 1.250$ g·cm^{-3}, $Z = 6$. Cell constants from a least-squares fit using 83 reflections up to $\theta = 45°$ and Cu Kα radiation. Bicapped hexagonal yellowish prism (0.23 × 0.50 mm) was used for the analysis.

(2.H$_2$O): $C_{12}H_{10}N_4O_2$·H$_2$O, M = 260.25, monoclinic, $I2/a$, $a = 16.0305$ (6) Å; $b = 12.5320$ (5) Å, $c = 13.2248$ (5) Å, $\beta = 107.163$ (3)°, $D_c = 1.362$ g.cm^{-3}, $Z = 8$, cell constants analogously as in 1, with 77 reflections, irregular transparent colorless sample (min 0.37 to max 0.50 mm).

(3): $C_9H_8N_2O_2$, M = 176.17, orthorhombic, $P2_12_12_1$, $a = 15.3173$ (7) Å, $b = 11.3889$ (4) Å, $c = 4.4948$ (2) Å, $D_c = 1.492$ g·cm^{-3}, $Z = 4$, cell constants from 68 reflections, colorless transparent prism (0.30 × 0.17 × 0.17 mm).

(4): $C_{12}H_{10}N_4O_2$, M = 242.24, monoclinic, $P2_1/c$, $a = 4.1602$ (3) Å, $b = 11.2272$ (9) Å; $c = 11.5409$ (14) Å, $\beta = 97.636$ (9)°, $D_c = 1.506$ g·cm^{-3}, $Z = 2$, cell constants from 54 reflections, colorless transparent prism (1.00 × 0.03 × 0.06 mm).

Data collection was analogous for all the compounds: Philips PW1100 diffractometer, Cu Kα radiation, graphite monochromator, $\omega/2\theta$ scans, bisecting geometry, 1 × 1° detector apertures, 1.5° scan width, 1 min per reflection, good stability, checked every 90 min. For compound **1**, a total of 3334 reflections was collected, giving rise to 892 independent ones (R_{int} = 0.012) and to 667 observed ones ($3\sigma(I)$ criterion for all compounds). For compound **2**, there were 2164 total data and 1807 observed ones. For compound **3**, we had 834 and 724 data, respectively, and for compound **4**, 794 and 661. No absorption corrections were considered necessary, the values being 6.58, 8.07, 8.57, and 8.49 cm^{-1}, respectively.

Structure Solution and Refinement. All structures were solved by direct methods[76] and refined by full-matrix least-squares procedures. All hydrogen atoms were located on a difference synthesis and refined iso-

(75) Elguero, J.; Jacquier, R. *Bull. Soc. Chim. Fr.* **1966**, 2832.

(76) Main, P.; Fiske, S. J.; Hull, S. E.; Lessinger, L.; Germain, G.; Declercq, J. P.; Woolfson, M. M.; *Multan 80 System*; University of York: England, **1980**.

750 *J. Am. Chem. Soc., Vol. 112, No. 2, 1990*

Catalán et al.

Chart I

1 R₃ = R₅ = Me
2 R₃ = R₅ = H

5 R₃ = R₅ = Me
3 R₃ = R₅ = H

6 R₃ = R₅ = Me
4 R₃ = R₅ = H

tropically. Compound **2** contains one water molecule of crystallization. An empirical weighting scheme was used, so as to give no trends in $\langle w\Delta^2 F\rangle$ versus $\langle|F_o|\rangle$ and $\langle \sin\theta/\lambda\rangle$. The final residual synthesis shows no peaks higher than 0.13, 0.26, 0.24, and 0.15 $e\text{Å}^{-3}$, respectively. Final R (R_w) factors were 0.035 (0.042), 0.046 (0.047), 0.082 (0.095), and 0.044 (0.050), respectively. Compounds **1** and **4** each contained half a molecule in the asymmetric unit. No attempt was made to analyze the absolute structure of compounds **1** and **3**. Most of the calculations were done with the XRAY76 system[77] on a VAX 11/750 computer. The atomic scattering factors were taken from the International Tables.[78]

Fluorescence and Phosphorescence Measurements. Room-temperature absorption spectra were obtained with a Perkin-Elmer 554 and a Shimadzu UV-265FS.

Fluorescence spectra at room temperature corrected for the instrumental sensitivity were measured with an SLM 48000$_\text{TM}$S spectrofluorometer by using a cooled wide band RF housing for the R928 photomultiplier tube. Corrected excitation spectra were obtained with constant excitation intensity controlled by a rhodamine B quantum counter in the reference channel. Fluorescence solutions were freshly prepared, and optical densities were measured in the excitation zone range of 0.02. Emission quantum yields were determined relative to that of quinine bisulfate in 0.1 M H_2SO_4[81] with appropriate corrections for the refractive indices of the solvents.[82]

Phosphorescence spectra corrected for the instrumental sensitivity, were measured with a Perkin Elmer Model LS5 spectrometer connected to the corresponding data station (Model 3600). Low-temperature emission studies were carried out employing a liquid nitrogen accessory to cool the samples to temperatures approaching 77 K.

A UV-Accelerometer device[83] was employed for the study of the photostability of the above compounds. The UV source consists of eight fluorescent tubes (Philips TL-40W) which have a wavelength range of 280–360 mm with max at 330 nm. The lamps are arranged vertically on the circumference of a drum around which samples rotate at a distance of 3.5 cm from the lamps. Solutions of the samples were irradiated in standard quartz cells, and their concentrations adjusted so that the same initial max absorbance (Abs = 0.2) was maintained. All the irradiations were conducted at 40 °C and used as a reference a sample of Tinuvin P simultaneously irradiated. The monitoring of sample photolysis was carried out by recording their full spectra at different times of irradiation. After the spectrophotometric readings, the samples were again placed in the UV-Accelerator and left to reach the equilibrium temperature (40 °C) before restarting irradiation.

Cyclohexane, ethanol, methanol, and dimethyl sulfoxide (Merck Uvasol grades) and acetonitrile (Scharlau HPLC grade) were used as
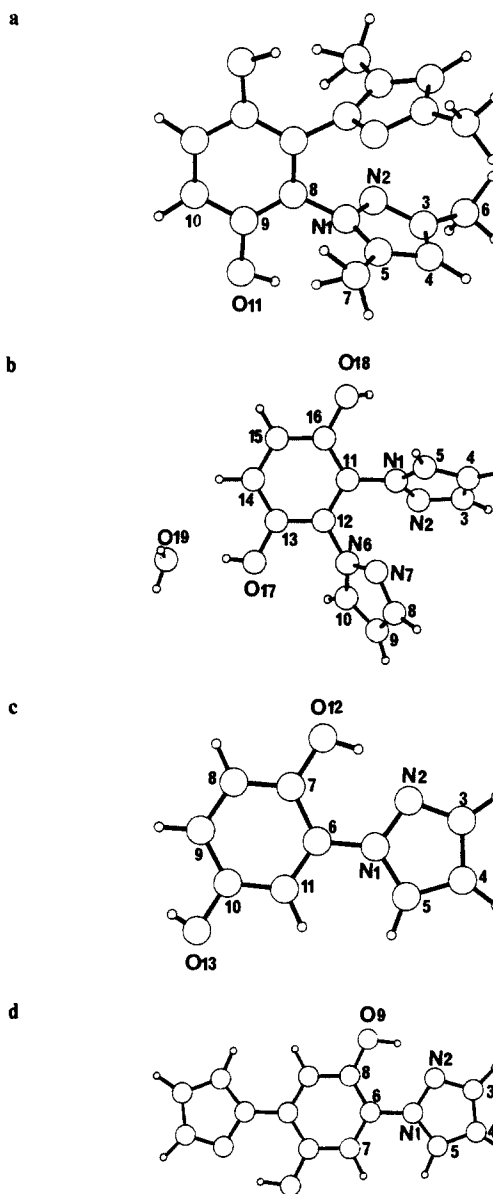
(77) Stewart, J. M.; Machin, P. A.; Dickinson, C. W.; Ammon, H. L.; Heck, H.; Flack, H. *The X-ray System*; Technical Report TR-446; Computer Science Center: University of Maryland, College Park, MD, 1976.

(78) *International Tables for X-ray Crystallography*; Kynoch Press: Birmingham, England, 1974; Vol. IV.

(79) Vainshtein, B. K.; Fridkin, V. M.; Indenbom, V. L. *Modern Crystallography II*; Springer: New York, 1982; p 87.

(80) Motherwell, W. D. S. PLUTO: *A Program for Plotting Crystal and Molecular Structures*; Cambridge University: England, 1978.

(81) Velapoldi, R. A.; Mielenz, K. D. *Standard Reference Materials: A Fluorescence Standard Reference Material Quinine Sulfate Dihydrate*; NBS. Spec. Publ. 260, January 1980.

(82) Demas, J. N.; Crosby, G. A. *J. Phys. Chem.* **1971**, *75*, 991.

(83) ASTM G-53-77 and UNE S3104.

a

b

c

d

Figure 2. The molecular structure[79] with the numbering used in the crystallographic work.

solvents for fluorescence and phosphorescence measurements.

Theoretical Calculations. INDO[84] fully optimized geometries have been used for ground-state calculations including the different conformations of compounds **1–4**. Proton-transfer curves in the ground state correspond to CNDO/2 calculations[84] in INDO fully optimized geometries of the planar systems with the only limitation being that of keeping the r_{OH} distance fixed during the optimization process. Calculations of electronic excited states, corresponding to the Franck–Condon approximation, have been obtained by using the CNDO/2 method with configuration interaction including the 60 monoexcited configurations of lower energy. Theoretical UV transitions have been calculated by CNDO/S[84] on fully INDO optimized geometries, considering also the 60 monoexcited configurations of lower energy.

Results and Discussion

Syntheses. Compounds **1, 2, 3, 4**, and **5** have been prepared by the synthetic method involving nucleophilic addition of N-unsubstituted pyrazoles to p-benzoquinone.

The only precedent in the literature for this type of reaction was reported by Grandberg and Kost[85] in 1959. These authors proposed structure **6** for the bis compound obtained from 3,5-

(84) *Modern Theoretical Chemistry*; Miller, W. H., Schaefer, H. F., Berne, B. J., Segal, G. A., Eds.; Plenum Press: New York, 1977; especially Vol. 7 and 8.

(85) Grandberg, I. I.; Kost, A. N. *Zh. Obshch. Khim.* **1959**, *29*, 1099.

Table I. Selected Geometrical Characteristics (Å, deg)[a]

compd	1	2	3	4
R	3,5-DiMePz	Pz	H	H
R'	H	H	H	Pz
R''	Me	H	H	H
N2-C3	1.323 (4)	1.330 (2), 1.327 (3)	1.325 (11)	1.332 (4)
C3-C4	1.389 (4)	1.392 (4), 1.385 (3)	1.403 (12)	1.383 (4)
C4-C5	1.373 (6)	1.362 (3), 1.362 (3)	1.358 (11)	1.361 (4)
C5-N1	1.345 (3)	1.349 (3), 1.349 (3)	1.375 (9)	1.363 (3)
N1-N2	1.375 (4)	1.358 (2), 1.352 (2)	1.368 (8)	1.361 (3)
N1-C6	1.427 (4)	1.424 (2), 1.422 (2)	1.400 (9)	1.425 (3)
C7-C8	1.392 (5)	1.386 (3), 1.391 (3)	1.363 (10)	1.383 (4)
C8-C9	1.356 (6)*	1.379 (3), 1.379 (3)	1.383 (11)	1.383 (3)
C10-C11	1.392 (5)	1.394 (2), 1.391 (2)	1.367 (10)	1.383 (4)
C7-O12	1.357 (4)	1.370 (2)	1.380 (9)	1.362 (3)
C10-O13		1.353 (2)	1.369 (9)	
N2-N1-C6	119.1 (2)	120.3 (1), 119.1 (2)	120.3 (6)	121.0 (2)
C5-N1-C6	128.4 (2)	127.9 (2), 128.6 (1)	128.5 (6)	128.6 (2)
N2-N1-C5	111.6 (3)	111.6 (1), 111.5 (1)	111.2 (6)	110.4 (2)
N2-C3-C4	110.5 (3)	111.2 (2), 111.9 (2)	111.3 (7)	111.6 (3)
C6-C7-O12	124.1 (4)	122.0 (2)	123.1 (6)	124.0 (2)
C8-C7-O12	118.2 (4)	119.3 (2)	117.4 (6)	117.2 (2)
C11-C10-O13		117.9 (2)	116.8 (6)	
C9-C10-O13		123.6 (2)	122.6	
N2-N1-C6-C7	99.8 (3)	-117.6 (2), -121.3 (2)	6.2 (10)	-6.8 (3)
C6-C7-O12-H12	-31 (3)	49 (2)	-3 (7)	7 (3)
C9-C10-O13-H13		-9 (2)	-4 (8)	

[a] The atomic numbering is referred to in the following scheme, so in **1** C10-C10' corresponds to C8-C9:
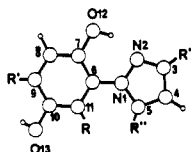
Table II. Selected Hydrogen Interactions (Å, deg)[a]

compd	X	Y	symmetry	X-H	X···Y	H···Y	X-H···Y
1	O11	N2	$x, x - y, {}^{7}/_{6} - z$	1.03 (5)	2.703 (4)	1.71 (4)	164 (4)*
1	C7	O11	$x - y + 1, 1 - y, 1 - z$	0.96 (5)	3.485 (5)	2.54 (5)	172 (7)
2	O17	O19	x, y, z	0.89 (4)	2.620 (2)	1.74 (4)	170 (3)*
2	O19	O18	$x, {}^{1}/_{2} - y, z - {}^{1}/_{2}$	0.90 (3)	2.870 (2)	2.02 (3)	157 (2)*
2	O19	N7	$1 - x, {}^{1}/_{2} + y, {}^{1}/_{2} - z$	0.89 (3)	2.792 (2)	1.91 (4)	171 (3)*
2	O18	N2	${}^{3}/_{2} - x, y, 1 - z$	0.91 (3)	2.717 (2)	1.81 (3)	173 (3)*
2	C15	O17	$x, {}^{1}/_{2} - y, {}^{1}/_{2} + z$	0.93 (3)	3.359 (2)	2.43 (3)	175 (2)
2	C10	O19	${}^{3}/_{2} - x, {}^{1}/_{2} - y, {}^{1}/_{2} - z$	0.98 (2)	3.360 (2)	2.70 (3)	125 (2)
3	O12	N2	x, y, z	0.99 (11)	2.558 (9)	1.74 (10)	138 (9)*
3	O13	O12	$-x, {}^{1}/_{2} + y, {}^{1}/_{2} - z$	0.97 (13)	2.742 (8)	1.80 (12)	162 (11)*
3	C5	O13	${}^{1}/_{2} - x, 1 - y, {}^{1}/_{2} + z$	1.04 (9)	3.250 (9)	2.25 (9)	162 (7)
4	O9	N2	x, y, z	0.91 (4)	2.612 (3)	1.79 (4)	149 (4)*
4	C4	O9	$x - 1, {}^{1}/_{2} - y, z - {}^{1}/_{2}$	0.99 (3)	3.356 (3)	2.62 (3)	131 (2)

[a] Those more likely[80] to be considered as hydrogen bonds are marked with an asterisk.

Table III. 1H NMR Spectroscopic Data[a,b]

compd	solvent	H3	H5	H6	OH1	OH4	H3'	H4'	H5'	Me3'	Me5'
1[c]	CDCl3		7.04 (s)	7.04 (s)	8.20 (s)	8.20 (s)		5.88 (s)		2.29 (s)	1.59 (s)
	DMSO-d6		6.95 (s)	6.95 (s)	9.28 (s)	9.28 (s)		5.68 (s)		1.94 (s)	2.02 (s)
2	CDCl3		7.05 (s)	7.05 (s)	8.31 (s)	8.31 (s)	7.82 (dd)	6.35 (dd)	6.84 (dd)		
							$J_{3',4'} = 1.8$	$J_{4',5'} = 2.5$			
							$J_{3',5'} = 0.7$				
	DMSO-d6		7.00 (s)	7.00 (s)	9.55 (s)	9.55 (s)	7.42 (dd)	6.21 (dd)	7.45 (dd)		
3	CDCl3	6.92 (d)	6.67 (dd)	6.97 (d)	10.92 (s)	4.68 (s)	7.73 (dd)	6.51 (dd)	7.95 (dd)		
		$J_{3,5} = 2.9$	$J_{5,6} = 8.7$				$J_{3',4'} = 1.9$	$J_{4',5'} = 2.5$			
							$J_{3',5'} = 0.7$				
	DMSO-d6	7.12 (d)	6.59 (dd)	6.85 (d)	9.81 (s)	9.11 (s)	7.70 (dd)	6.48 (dd)	8.36 (dd)		
4	CDCl3	7.14 (s)		7.14 (s)	11.16 (s)	11.16 (s)	7.74 (d)	6.53 (dd)	7.98 (d)		
							$J_{3',4'} = 1.9$	$J_{4',5'} = 2.5$			
	DMSO-d6	7.47 (s)		7.47 (s)	10.17 (s)	10.17 (s)	7.73 (d)	6.50 (dd)	8.41 (d)		
5	CDCl3	6.75 (d)	6.69 (dd)	6.96 (d)	9.28 (s)	3.75 (s)		6.03 (s)		2.29 (s)	2.41 (s)
		$J_{3,5} = 2.9$	$J_{5,6} = 8.8$								
	DMSO-d6	6.57 (d)	6.67 (dd)	6.80 (d)	9.18 (s)	9.04 (s)		5.93 (s)		2.13 (s)	2.07 (s)

[a] Chemical shifts, δ in ppm, and coupling constants, J in Hz. [b] s = singlet and d = doublet. [c] Assignment of the Me3' and Me5' has been checked by heteronuclear (1H-13C) 2D correlations with a J value of 150 Hz.
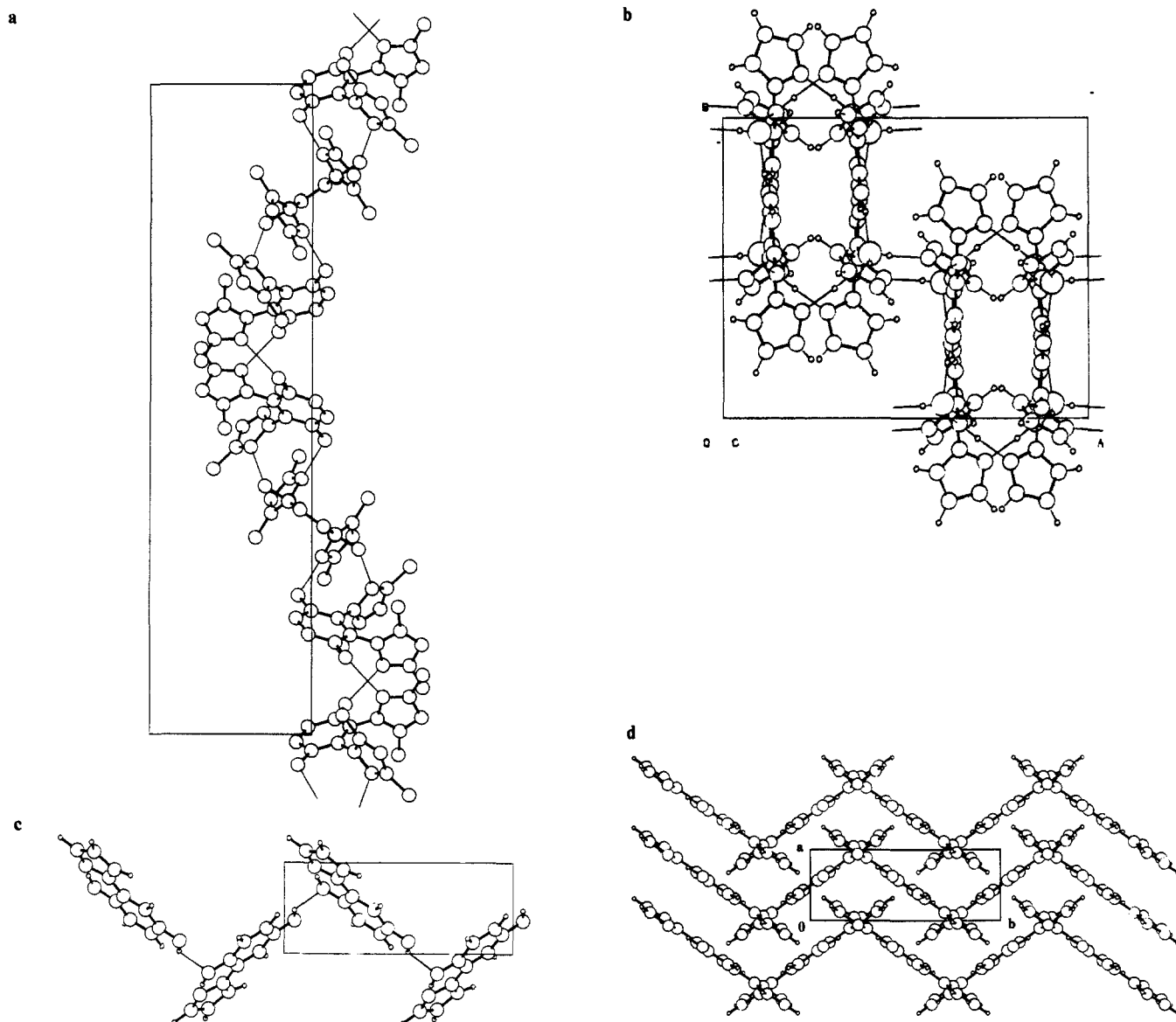
a

b

c

d

Figure 3. The packing of the molecules in the four compounds 1-4.

dimethylpyrazole and *p*-benzoquinone on the basis of elemental analysis only and the reasonable assumption that it should be the less hindered isomer. In fact, we have been able to prove by the spectroscopic techniques (Tables III and IV) and X-ray crystallography that the main product formed in this reaction is the isomer 1 and that a small percentage of the monoadduct 5 is also formed. No traces of derivative 6 could be detected in the crude reaction product.

Reaction of pyrazole itself with *p*-benzoquinone afforded three compounds 2, 3, and 4 which were fully characterized (see Tables III and IV).

A study of the mechanism of the nucleophilic addition of pyrazole to *p*-benzoquinone and of the influence of substituents on the selectivity is now in progress and will be the subject of a future paper.[86]

X-ray Crystallography (Compounds 1, 2, 3 and 4). The main geometrical characteristics derived for the four molecules (1-4) are given in Table I; Figure 2a-d shows the spatial relationship between the different parts of the respective molecules. In all compounds, the double bonds of the pyrazole ring are located at N2-C3 and C4-C5, with intracyclic bond angles at N1 and C3 greater than other angles within the ring. It will be noticed that the exocyclic angle C5-N1-C(Ph) is larger than the N2-N1-C-

(Ph) angle. In particular, C3-C4 possesses some resonant character in molecule 4, while in 1 the C4-C5 double bond is somehow delocalized in the C5-N1 bond.

The phenyl ring in compound 3 has some quinone character with small values for the C7-C8 and C10-C11 bond lengths, and in compound 1 C10-C10' is the shortest bond, probably due to thermal motion. Again, molecule 3 presents the shortest N1-C6 bond.

As far as the OH groups are concerned, they present, in all cases, different values for the two C-C-O angles within each compound, being greater that one on the H-bond side. The conformation about the OH hydrogen atom is described by the C-C-O-H torsion angle (see Table I).

The relative position of the pyrazole ring of each compound, with regard to the phenyl ring, is shown in Table I by means of the C-C-N-N torsion angle. In compound 1, both pyrazole rings make an angle of 84.3 (1)° with the phenyl ring, while in compound 2 they make angles of 64.3 (1) and 59.6 (1)°. The angle between the two pyrazole rings is 40.2 (1) and 47.1 (1)° for compounds 1 and 2, respectively.

Figure 3a-d and Table II describe the interactions involving the OH groups that determine the packing of the crystals.

Compound 3 presents the H-bonds connecting molecules in a helix system along the 2-fold axis parallel to *b*.

Compound 1 also presents a helix system but around the 6-fold screw axis parallel to *c*. The helix packs inside the phenyl rings

(86) Santa María, D.; Ballesteros, P.; Claramunt, R. M. Unpublished results.

Photoinduced Intramolecular Proton Transfer

J. Am. Chem. Soc., Vol. 112, No. 2, 1990 753

Table V. Substituted Phenols: Chemical Shifts (δ H) in ppm Downfield from Internal TMS and Electronic Populations Localized on the Hydrogen Atom (q_H)

substituent	δ H (CCl$_4$)	δ H (DMSO-d_6)	q_H
H	4.29	9.23	0.8504
2-F		9.70	0.8458[a]
2-CF$_3$		10.44	0.8393[a]
2-OMe		8.76	0.8494[a]
2-NO$_2$		10.80	0.8416[a]
3-NO$_2$		10.37	0.8404[b]
3-Me		9.15	0.8508[b]
3-NH$_2$		8.77	0.8517[b]
4-F	4.20	9.33	0.8485[b]
4-OMe	3.97	8.80	0.8519[b]
4-NO$_2$	5.16	10.90	0.8390[b]
4-Me	4.10	9.03	0.8506[b]
4-NH$_2$		8.28	0.8543[b]
4-OH		8.55	0.8525[b]
4-CO$_2$Me		10.24	0.8425[b]
4-CHO		10.57	0.8439[b]

^{a} q_H calculated values for the OH trans conformer. ^{b} Mean value of the q_H calculated values for the OH cis and trans conformers.

and outside the pyrazole ones. This results in a core of phenyl C atoms, then a sheet of O atoms, followed by the N atoms of the pyrazole ring, and leaving on the outside the C atoms of the pyrazole ring.

Compound **4** packs with intercrossing sheets of parallel molecules stacked along the (1 2 0) and (1 $\bar{2}$ 0) rational planes (which correspond to the strongest reflections of the structure).

All of these quite regular packings are destroyed in the crystal **2** due to the presence of the water molecule which is involved in the hydrogen bonding scheme and produces a three-dimensional network.

Only in compounds **3** and **4**, are there intramolecular H-bonds, one bond in **3** and two bonds in **4**.

Spectroscopy. In Tables III and IV are gathered the ^{1}H and ^{13}C NMR spectroscopic data for compounds **1–5**. The assignment of the signals to the different heterocyclic protons was made with 1-methylpyrazole and 1,3- and 1,5-dimethylpyrazole as model compounds.[87] For the protons of the 1,4-dihydroxybenzene nucleus, the multiplicity of the signals and coupling constant values were considered. Careful analysis of the satellite bands due to isotopomers that would appear as doublets around the unique signal for aromatic protons H$_5$–H$_6$ in compounds **1** and **2** and H$_3$–H$_6$ in product **4** allowed us to evaluate the coupling constants H$_5$–^{13}C–^{12}C–H$_6$ $\sim$ 9 Hz and H$_3$–^{13}C–^{12}C–H$_6$ $\sim$ 0 Hz. These values can be used in the future to distinguish between the two series of isomeric but symmetrical derivatives.

Because the 1-OH phenolic protons of derivatives **3** and **4** are involved in an intramolecular hydrogen bond, they occur at lower field than do other phenolic protons (e.g., the 4-OH protons of derivatives **3** and **5**) which are not so involved; the shifts of the latter protons are solvent dependent changing from 4.2 ppm in CDCl$_3$ to 9.1 ppm in DMSO-d_6.

On the contrary, for the OH groups in 2,3-bis(3′,5′-dimethylpyrazol-1′-yl)- and 2,3-bis(pyrazol-1′-yl)-1,4-dihydroxybenzenes **1** and **2** have intermediate values which range between 8.2 and 9.6 ppm, depending on the solvent.

The ^{1}H NMR spectra of compounds 2-(pyrazol-1′-yl)-1,4-dihydroxybenzene (**3**), 2,5-bis(pyrazol-1′-yl)-1,4-dihydroxybenzene (**4**), and TIN have also been recorded in acetonitrile-d_3 containing a small drop of absolute ethanol; the chemical shifts of the OH hydrogen-bonded protons remained unchanged with values of 10.92, 11.16, and 11.10 ppm, respectively.

From the literature data for the hydroxyl ^{1}H NMR chemical shifts in DMSO-d_6 solution of 16 ortho-, meta-, and para-substituted phenols[88] and the corresponding electron population of

(87) (a) Elguero, J. In *Comprehensive Heterocyclic Chemistry*; Katritzky, A. R., Rees, C. W., Eds.; Pergamon: Oxford, 1984; Vol. 5, p 167. (b) Batterham, T. J. *NMR Spectra of Simple Heterocycles*; Wiley: New York, 1973; p 173.

(88) Tribble, M. T.; Traynham, J. G. *J. Am. Chem. Soc.* **1969**, *91*, 379.

Table IV. ^{13}C NMR Spectroscopic Data in DMSO-d_6^{a,b}

compd	C$_1$	C$_2$	C$_3$	C$_4$	C$_5$	C$_6$	C$_3'$	C$_4'$	C$_5'$	Me$_3'$	Me$_5'$
1	146.5 (ddd) $^3J = 11.5$ (H$_3$) $^2J = 3.8$ (H$_6$) $^2J = 7.7$ (OH)	125.7 (br s)	125.7 (br s)	146.5 (ddd) $^3J = 11.5$ (H$_6$) $^2J = 3.0$ (H$_5$) $^2J = 7.7$ (OH)	117.1 (d) $^1J = 161.2$	117.1 (d) $^1J = 161.2$	146.5 (masked)	103.7 (dqq) $^1J = 172.0$ $^3J = 3.0$ (Me$_5'$) $^3J = 3.0$ (Me$_3'$)	141.4 (dq) $^2J = 7.1$ (Me$_5'$) $^3J = 7.1$ (H$_4'$)	13.3 (q) $^1J = 127.2$	10.8 (q) $^1J = 127.5$
2	145.6 (ddd) $^3J = 11.4$ (H$_3$) $^2J = 4.4$ (H$_6$) $^2J = 7.0$ (OH)	125.2 (br s)	125.7 (br s)	145.6 (ddd) $^3J = 11.4$ (H$_6$) $^2J = 4.4$ (H$_5$) $^2J = 7.0$ (OH)	117.1 (d) $^1J = 162.6$	117.1 (d) $^1J = 162.6$	139.4 (ddd) $^1J = 184.5$ $^2J = 5.4$ (H$_4'$) $^3J = 9.1$ (H$_5'$)	105.4 (ddd) $^1J = 177.3$ $^2J = 9.3$ (H$_3'$) $^2J = 9.3$ (H$_5'$)	132.5 (ddd) $^1J = 189.8$ $^2J = 9.1$ (H$_4'$) $^3J = 5.5$ (H$_3'$)		
3	140.8 (ddd) $^3J = 9.5$ (H$_3$) $^3J = 6.9$ (H$_5$) $^2J = 2.6$ (H$_6$)	127.0 (ddd) $^3J = 7.5$ (H$_6$) $^2J = 2.6$ (H$_3$) $^3J = 4.9$ (OH)	109.0 (dd) $^1J = 160.4$ $^3J = 5.2$ (H$_5$)	150.2 (ddd) $^3J = 10.5$ (H$_6$) $^2J = 3.2$ (H$_5$) $^2J = 3.2$ (H$_3$)	114.3 (d) $^1J = 160.5$ $^3J = 5.9$ (H$_3$)	118.1 (d) $^1J = 159.9$	139.4 (ddd) $^1J = 186.1$ $^2J = 6.0$ (H$_4'$) $^3J = 8.5$ (H$_5'$)	106.5 (ddd) $^1J = 177.4$ $^2J = 10.4$ (H$_3'$) $^3J = 9.0$ (H$_5'$)	130.7 (ddd) $^1J = 191.7$ $^2J = 9.6$ (H$_4'$) $^3J = 4.6$ (H$_3'$)		
4	140.7 (ddd) $^3J = 11.0$ (H$_3$) $^2J = 3.7$ (H$_6$) $^2J = 7.1$ (OH)	125.4 (dd) $^3J = 9.0$ (H$_6$) $^3J = 5.2$ (OH)	111.0 (d) $^1J = 162.8$	140.7 (ddd) $^3J = 11.0$ (H$_6$) $^2J = 3.7$ (H$_3$) $^2J = 7.1$ (OH)	125.4 (dd) $^3J = 9.0$ (H$_3$) $^3J = 5.2$ (OH)	111.0 (d) $^1J = 162.8$	139.5 (ddd) $^1J = 185.6$ $^2J = 5.1$ (H$_4'$) $^3J = 9.2$ (H$_5'$)	106.5 (ddd) $^1J = 177.7$ $^2J = 9.7$ (H$_4'$) $^2J = 9.7$ (H$_5'$)	130.9 (ddd) $^1J = 191.7$ $^2J = 8.7$ (H$_4'$) $^3J = 3.9$ (H$_3'$)		
5	144.5 (ddd) $^3J = 9.4$ (H$_3$) $^3J = 6.9$ (H$_5$) $^2J = 2.5$ (H$_6$)	127.0 (br s)	114.6 (ddd) $^1J = 159.9$ $^3J = 4.9$ (H$_5$) $^3J = 4.9$ (OH)	149.8 (ddd) $^3J = 7.3$ (H$_6$) $^2J = 3.0$ (H$_3$) $^2J = 3.0$ (H$_5$)	116.2 (ddd) $^1J = 159.9$ $^3J = 4.8$ (H$_3$) $^3J = 4.8$ (OH)	117.5 (d) $^1J = 159.5$	147.2 (dq) $^2J = 6.1$ (Me$_5'$) $^2J = 6.1$ (H$_4'$)	105.0 (dqq) $^1J = 172.9$ $^3J = 3.5$ (Me$_3'$) $^3J = 3.5$ (Me$_5'$)	143.6 (dq) $^2J = 7.0$ (Me$_5'$) $^2J = 7.0$ (H$_4'$)	13.4 (q) $^1J = 126.6$	11.2 (q) $^1J = 128.4$

^{a} (Chemical shifts, δ in ppm, and coupling constants, J in Hz.) ^{b} br = broad, s = singlet, d = doublet, q = quartet.

754 *J. Am. Chem. Soc., Vol. 112, No. 2, 1990*

Catalán et al.

^2J (C$_1$-OH) =n.o. ^2J(C$_1$-OH)= 7.0-7.7 ^2J(C$_1$-OH)= 7.1

^3J (C$_7$-OH) =4.9 ^3J(C$_7$-OH)= n.o. ^3J(C$_2$-OH)= 5.2
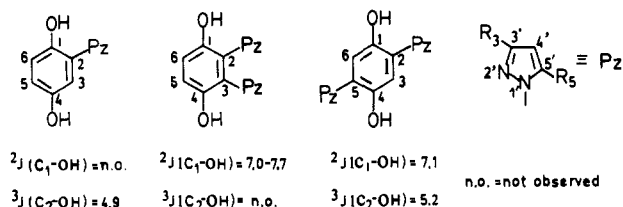
n.o. =not observed

Figure 4. Averaged values of coupling constants between benzene carbon atoms and protons of the phenol groups through two and three bonds, ^2J and ^3J in Hz.

the hydrogen atom, q_H, calculated by the INDO method[89] (Table V), we have obtained the following relationship:

$$\delta_H = 146.0 - 161.1 q_H \qquad n = 16; \; r^2 = 0.92$$

The fact that this equation is also valid for the ortho-substituted phenols shown in Table V excludes the possibility that such compounds possess an IMHB in DMSO solution. In DMSO, all the phenols studied form an intermolecular hydrogen bond with the solvent. With our pyrazole derivatives, q_H (0.844) could be calculated for the bis derivative **2**; δ_H calc was 10.0 ppm and δ_H exptl 9.55 ppm. Because the bis derivative **1** has too many atoms, q_H and δ_H were not calculated, but their values would be close to those obtained for the bis compound **2**. With compounds **3** and **4**, the IMHB existing between the pyrazole N-2 nitrogen atom and the adjacent phenolic groups is not disrupted by DMSO.

A similar correlation for ortho-substituted phenols in carbon tetrachloride[90] can also be established:

$$\delta_H = 79.4 - 88.5 q_H \qquad n = 5; \; r^2 = 0.96$$

In this case, the resonance positions of the hydroxyl proton in dilute solution indicate the relative amount of IMHB since in dilute solutions only monomers are expected to exist. For the following compounds 2-(2'-hydroxyphenyl)benzoxazole (HPBO), q_H = 0.763, δ_{Hcalc}= 11.9, δ_{Hexp} = 11.15; 2-(2'-hydroxy-5'-methylphenyl)benzotriazole (TIN), q_H = 0.767, δ_{Hcalc} = 11.5, δ_{Hexp} = 11.10; 2-(pyrazol-1'-yl)-1,4-dihydroxybenzene (**3**), q_H = 0.779, δ_{Hcalc} = 10.4, δ_{Hexp} = 10.92; and 2,5-bis(pyrazol-1'-yl)-1,4-dihydroxybenzene (**4**), q_H = 0.778, δ_{Hcalc} = 10.5, δ_{Hexp} = 11.16, the hydroxyl resonance did not vary with the concentration thus indicating strong intramolecular hydrogen bonding. For 2,3-bis(pyrazol-1'-yl)-1,4-dihydroxybenzene (**2**) the δ_H of the phenol group is anomalously large and does not vary with concentration.

The assignments of the ^{13}C NMR chemical shifts to the pyrazole ring carbon atoms of compounds **1–5** and measurement of the ^{13}C–^{1}H coupling constants were achieved using reference data for 1-methylpyrazole and 1,3,5-trimethylpyrazole.[91,92] ^{13}C NMR chemical shifts of the 1,4-dihydroxybenzene nucleus have been assigned by taking into account the influence of the pyrazole substituents and multiplicity of the signals.

Heteronuclear (^{1}H–^{13}C) 2D-correlation experiments with J values of 166, 10, 7, and 3 Hz in compound **3** confirmed the assignments. Interesting observed features were the coupling constants between some carbons and the proton of the OH group as shown in Figure 4: such coupling has seldom been reported.[93]

Theoretical and Photophysical Studies of Tinuvin P. Singlet States. The electronic spectra of 2-(2'-hydroxyphenyl)benzotriazoles **II**, including Tinuvin P, consist of two broad overlapping bands located at about 300 and 340 nm (in chloroform and in heptane).[1] Nonplanar 2-(4'-hydroxyphenyl)benzotriazoles, e.g., the 3-methyl derivative, absorb at 325 nm, whereas hindered ones, e.g., the 2-methyl derivative, absorb at 297 nm (like 2-phenyl-benzotriazole itself, λ_{max} = 308 nm).[1] From these results, it was

(89) Catalan, J.; Macias, A. *J. Chem. Soc., Perkin Trans. 2* **1979**, 1632.

(90) Seguin, J. P.; Guillaume-Vilport, F.; Uzan, R.; Doucet, J. P. *J. Chem. Soc., Perkin Trans. 2* **1986**, 773.

(91) González, E.; Faure, R.; Vincent, E. J.; Espada, M.; Elguero, J. *Org. Magn. Reson.* **1979**, *12*, 587.

(92) Bruix, M.; Claramunt, R. M.; Elguero, J.; de Mendoza, J.; Pascual, C. *Spectrosc. Lett.* **1984**, *17*, 757.

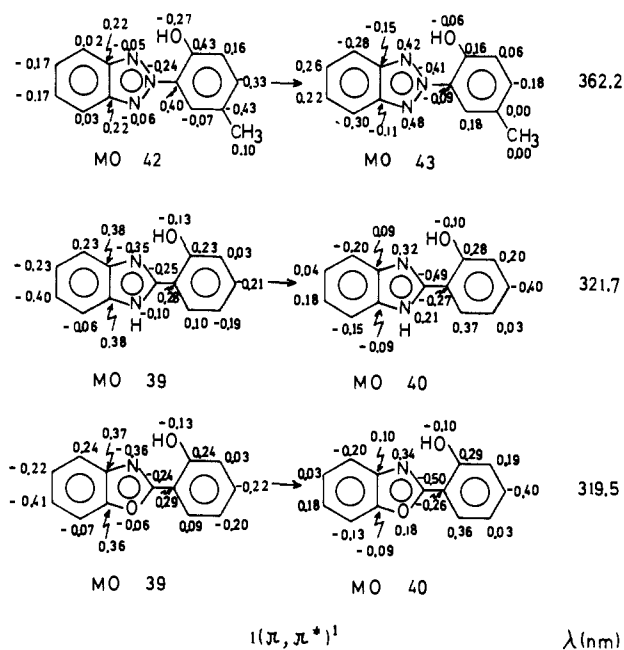(93) Breitmaier, E.; Voelter, W. In *Carbon-13 NMR Spectroscopy*, 3rd ed.; VCH: New York, 1987.

Table VI. CNDO/S//INDO CI Calculations (with Mataga Type Integrals) for Tinuvin P

state	λ(nm)	f	α^a (deg)	μ^* (D)
$1(n.\pi^*)^1$	365.9			3.92
$1(\pi.\pi^*)^1$	362.2	0.26	3.13	9.39
$2(\pi.\pi^*)^1$	306.1	0.08	74.37	8.36
$3(\pi.\pi^*)^1$	298.4	0.05	157.25	7.36
$1(\pi.\pi^*)^3$	816.0			1.91
$2(\pi.\pi^*)^3$	517.6			3.40

^{a}The angle has been defined according to the following criterium:
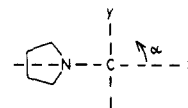
concluded[60] that compounds **II** exist as a mixture of planar IMHB (responsible for the 340-nm absorption) and nonplanar (300-nm band) conformations.

This widely accepted model[71-74] has been recently challenged by Wössner et al.[51] who showed that the ratio of the intensities of the two UV maxima in TIN is independent of the viscosity and temperature.

Our CNDO/S calculations on Tinuvin P (Table VI) also show that the planar structure predicts transitions at 362 and 306 nm and therefore explains the two UV absorption maxima actually observed; however, it does not explain why these maxima are (i) so large and (ii) have no fine structure in inert solvents. Besides, the transition at 362 nm corresponds to a highly polar excited state, possessing a dipole moment (μ_s^*) of 9.4 D. It would be expected that this transition should be shifted to the red when the refractive index of the solvent increased, but the experimental data[1,60] do not confirm this.

This theoretical explanation for the origin of the first $\pi \rightarrow \pi^*$ transition in the UV spectrum of Tinuvin P can also be applied to the same transitions observed in the spectrum of 2-(2'-hydroxyphenyl)benzimidazole (HPBI) and in that of 2-(2'-hydroxyphenyl)benzoxazole (HPBO). These observed transitions are calculated to correspond to μ_s^* = 10.9 and μ_s^* = 9.5 D, respectively. If we analyze the origin of these highly polar excited states, it can be calculated that the long wavelength absorption of Tinuvin P corresponds to 91% of the transition occurring between the molecular orbitals 42 $\rightarrow$ 43. This result implies a charge transfer of 0.54e$^-$ from the phenolic ring to the benzotriazole ring. In HPBI and HPBO, the long wavelength absorptions correspond to 93% of the transition between the molecular orbitals 39 $\rightarrow$ 40, but, for these two compounds, the charge transfer occurs in the opposite direction, i.e., from the heterocyclic ring to the phenolic ring; however, the values calculated are only 0.26e$^-$ and 0.23e$^-$, respectively.

One could conclude from these results that in Tinuvin P the high μ_s^* is mainly a consequence of the charge transfer, whereas in the benzimidazole and benzoxazole derivatives, the high μ_s^* is due to charge variations in the distant positions 4 and 6 arising from this electronic transition $\pi \rightarrow \pi^*$.

The analysis of the molecular orbitals implicated in the transition lead us to conclude that in the three derivatives the 2-1' union is always strongly nonbonding in the π orbital, but is bonding in the π^* of HPBI and HPBO molecules and on the contrary remains antibonding in the π^* of Tinuvin P, indicating therefore that the rotation of the phenol group should be favored in the $1(\pi,\pi^*)^1$ of the Tinuvin P system. In Figure 6, we present the results corresponding to the three compounds TIN, HPBI, and HPBO, and clearly less energy is required to rotate the phenolic ring of Tinuvin P out of the plane of the benzotriazole ring than it does to perform the same operation for HPBI and HPBO. This is consistent with the experimental observation (Figure 7) that the first UV band of the benzotriazole derivative shows the lower resolution.

So we can end this theoretical study of stating the TIN probably exists as an equilibrium of conformations, i.e., planar (see Table VI) and other ones slightly nonplanar. Our conclusions are in

Photoinduced Intramolecular Proton Transfer

J. Am. Chem. Soc., Vol. 112, No. 2, 1990 755

Figure 5. Coefficients for the $2p_z$ orbitals in molecular orbitals implicated in the $1(\pi,\pi^*)^1$ transition for TIN, HPBI, and HPBO.
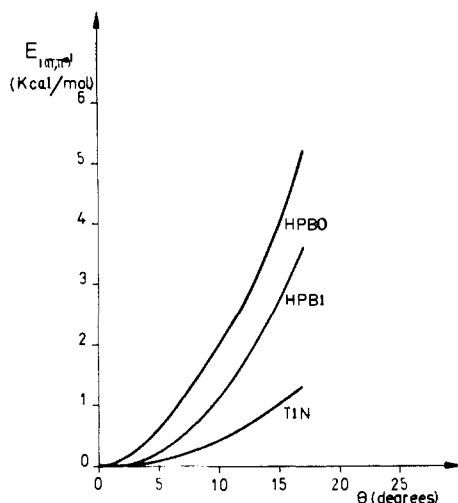

Figure 6. Energy variation in kcal/mol of the $1(\pi,\pi^*)^1$ transition with phenol group rotation. (θ is the torsion angle between the heterocycle and the phenol planes.)

agreement with the proposals of Heller[1] and of Goeller et al.[68]

Triplet States. In 1979 Werner[7] found that in Tinuvin P in methylcyclohexane/isopentane did not emit phosphorescence even at low temperature (90 K). From quenching experiments he was able to fix the T_1 of TIN at 60 ± 1 kcal/mol referring to the ground state, and by means of triplet energy transfer experiments in three stages (thioxanthone/Tinuvin P/anthracene) he deduced that the half-life of this triplet was less than 20 ns. Werner tried to explain this anomalous short half-life by assuming (i) that the quinonoid form has a triplet having approximately the same energy as the phenolic form and that it could be readily transformed to the latter form or (ii) because there was a rapid intersystem crossing (ISC) to the ground state.

Out theoretical calculations predict that, in the zone of 60 ± 1 kcal/mol, there is a triplet π,π^* (55.3 kcal/mol) that is T_2 and not T_1. The theoretical prediction for Tinuvin P with a T_1 at 35 kcal/mol (820 nm) was completely unexpected; moreover this T_1 arises from the $2(\pi,\pi^*)^1$, conferring a splitting S-T of 20400 cm^{-1}. A similar situation has neither been found in HPBI with a T_1 at 473 nm nor in HPBO with a T_1 at 475 nm.

In the light of experimental data, we can now proceed to analyze the viability of this triplet. The triplet quenching experiments
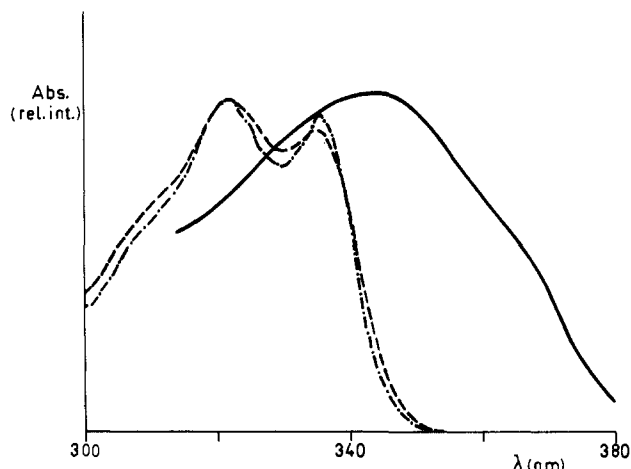

Figure 7. First band of the UV absorption spectra of TIN (—), HPBI (–·–), and HPBO (–) in cyclohexane.

done by Werner in benzene at room temperature using xanthone (74), thioxanthone (65.5), 4,4-bis(dimethylamino)benzophenone (62), benzoylbiphenyl (61), 5-methyl-2-naphthyl ketone (59), and 6-methyl-1-naphthyl ketone (56) as donors and Tinuvin P as acceptor clearly indicated that TIN has a triplet at 60 ± 1 kcal/mol but did not exclude the existence of a triplet of much less energy ($\sim$25 kcal/mol less) if we consider too that the data corresponding to coronene (54.4) and fluoranthene (53) surprisingly increase the quenching constant.

Besides, kinetic studies with the thioxanthone/Tinuvin P/ anthracene system allowed Werner to estimate from the temporal reliance of anthracene triplets that the quenching constants of TIN and thioxanthone by anthracene itself can be expressed as

$$k_{q3A}[A] - k_{q3B}[\text{Tinuvin P}] - k_{q3D}[\text{thioxanthone}] = k_A$$

In Werner's experimental conditions this becomes

$$3.2 \times 10^{-3}k_{q3A} + 7.4 \times 10^{-3}k_{q3B} + 5.9 \times 10^{-2}k_{q3D} = 2.8 \times 10^{-6} \text{ s}^{-1}$$

If a triplet at 35 kcal/mol in Tinuvin P exists, it seems reasonable that the triplet quenching of anthracene would be practically controlled by thioxanthone and the autoquenching could be neglected in a first approximation. So the latter mathematical equation converts to

$$k_{q3B} = \frac{2.8 \times 10^6}{7.4 \times 10^{-3}} \simeq 4 \times 10^8$$

Anthracene with a triplet of 42 kcal/mol is quenched with a quenching constant higher than that found for fluoranthene with a triplet at 53 kcal/mol, so indicating that in Tinuvin P a triplet of less energy should exist.

In order to check this possibility we carried out the following experiment: when an air-equilibrated solution of anthracene at 25 °C in methanol was excited in the zone range of 500–580 nm, a luminescence near 800 nm was detected due to the T_1 anthracene triplet[94] with a half-life of 0.005 ms. In Figure 8 it can also be seen that this luminescence was quenched significantly by Tinuvin P.

A Stern–Volmer treatment of the data obtained afforded the following expression:

ϕ_0/ϕ	Q	
1	0	
1.71	7.09×10^{-5}	$\phi_0/\phi = 0.93 + 1.28 \times 10^4 [Q]$; $R^2 = 0.98$
2.82	1.42×10^{-4}	

From the slope value of 1.28×10^4 and assuming that τ_A in ethanol and in methanol have the same value of 5×10^{-6} s we

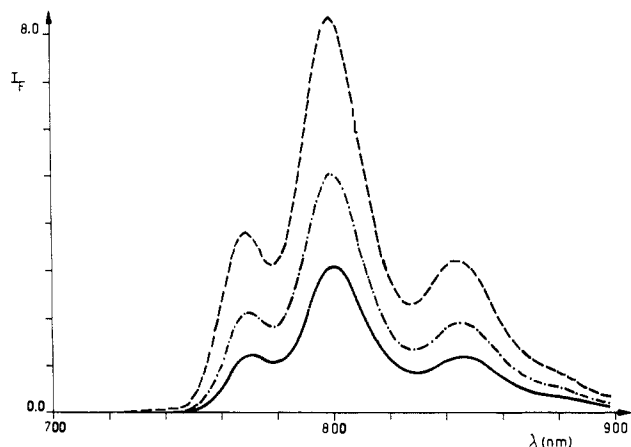(94) Turro, N. J. In *Modern Molecular Photochemistry*; Benjamin: New York, 1978; p 94.

756 *J. Am. Chem. Soc., Vol. 112, No. 2, 1990*

Catalán et al.

Figure 8. Luminescence quenching of the anthracene triplet at 800 nm by Tinuvin P: (- -) anthracene, 3.7×10^{-4} M; (-·-) anthracene, 3.7×10^{-4} M/TIN, 7.0×10^{-5} M; (—) anthracene, 3.7×10^{-4} M/TIN, 1.4×10^{-4} M.

can conclude that the quenching constant k_q is approximately 2.56 $\times 10^9$, thus it is controlled by diffusion ($k_{difMeOH}$ 25 °C = 1 $\times 10^{10}$).[7] This result supports the hypothesis that Tinuvin P has an electronic state beyond 800 nm toward the red which enables it to accept the anthracene luminescence. The existence of this triplet explains the short half-life (<20 ns) found by Werner[7] merely as a process of internal conversion (IC) to the T_1, which really exists in this time scale.

Proton Transfer. There is a key question in the problem that we have been considering all through the paper: Why at room temperature is it only possible to detect a slight fluorescence in crystalline Tinuvin P, whereas in 2-(2'-hydroxyphenyl)benzoxazole and 2-(2'-hydroxyphenyl)benzimidazole the fluorescence can be observed even in solution of an inert solvent and in some of them with high quantum yields? So, for HPBI in cyclohexane, the quantum yield is $\phi_F = 0.5$.[59] The answer actually accepted is that, according to the Ottersted model,[5] the quinonoid form presents an efficient nonradiative process which extinguishes this emission, and, as explained in the Introduction of the present paper, it is this process which is thought to be responsible for the photostability of 2-(2'-hydroxyphenyl)benzotriazoles.

In the photophysics of 2-(2'-hydroxyphenyl)azoles, the main problem is to know which percentage of electronically excited molecules evolves from the photogenerated Franck–Condon state to the quinonoid state $1(\pi,\pi^*)^1$. The fluorescence quantum yield of this latter form is given by the product between the efficiency to produce this state ϕ_{TP} and the intrinsic fluorescence quantum yield of this form ϕ_F^C.

$$\phi_F = \phi_{TP} \cdot \phi_F^C; \quad \phi_{TP} = \frac{\phi_F}{\phi_F^C} = \frac{\phi_F}{\tau_F^C \cdot k_F^C}$$

The fluorescence radiative constant k_F^C cannot be calculated from the absorption spectra due to the nonexistence of this quinonoid form in the ground state and must be estimated from half-time measurements τ_F^C at low temperature with the hypothesis that the only kinetic decay temperature that is independent is the radiative one, so

$\phi_{TP}(\text{room temperature}) \simeq$

$$\frac{\phi_F(\text{room temperature}) \times \tau_F^C(\text{low temperature})}{\tau_F^C(\text{room temperature})}$$

We have enough experimental evidence from the literature to study this problem in the cases of HPBO and TIN. In this way for the 2-(2'-hydroxyphenyl)benzoxazole

$\phi_F(300 \text{ K}) = 0.018^{32}$

$\tau_F^C(300 \text{ K}) = 0.2\text{ns}^{32} \quad \phi_{TP}(300 \text{ K}) = 0.5$
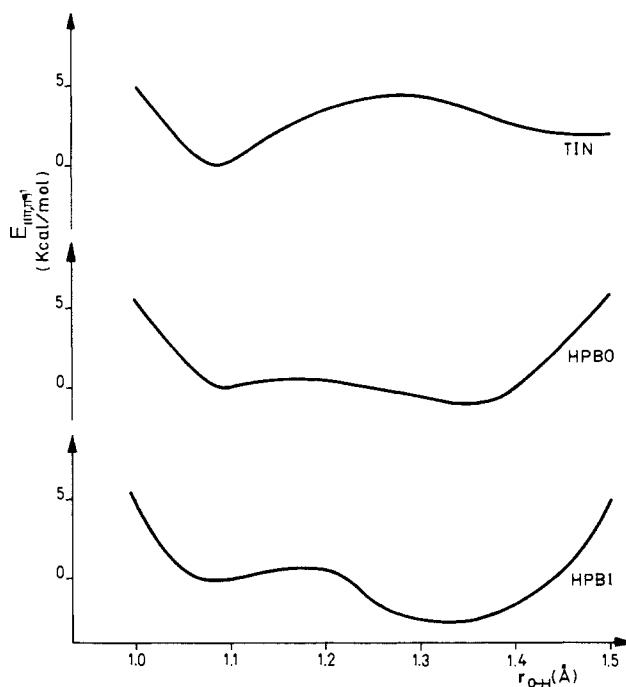
$\tau_F^C(77 \text{ K}) = 5.6\text{ns}^{32}$

Figure 9. Proton-transfer Franck–Condon curves for $1(\pi,\pi^*)^1$ of planar TIN, HPBI, and HPBO.

As a first approach to the problem we can conclude from this result that in the HPBO system at least 50% of the generated Franck–Condon molecules produce a state that emits red fluorescence at 490 nm.

For TIN we have

$\phi_F(300 \text{ K}) = 0.000018^{95}$

$\tau_F^C(300 \text{ K}) = 141 \text{ ps}^{44} \quad \phi_{TP}(300 \text{ K}) = 1.7 \times 10^{-4} \simeq 0.0002$

$\tau_F^C(12 \text{ K}) = 1.33 \text{ ns}^{68}$

Hence only two molecules of every 10 000 electronically excited ones would be expected to be energetic enough to undergo proton transfer, i.e., to give the quinonoid form if there is no K_{nr} temperature independent. This result also explains why there is no observed fluorescence in Tinuvin P.

To clarify this point we have calculated, in a similar way as we did for salicylates[11,14,47] or 7-azaindole,[96] the corresponding proton-transfer curves in $1(\pi,\pi^*)^1$ for the three planar molecules Tinuvin P, HPBO, and HPBI that are assembled in Figure 9. These results support all statements made before and point out that the quinonoid form in TIN is more unstable than the phenol one in the $1(\pi,\pi^*)^1$ state, whereas the opposite is the case for HPBO and HPBI.
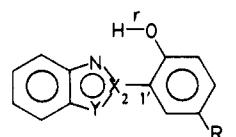
As explained already, from the molecular orbitals of the transition $1(\pi,\pi^*)^1$ it could be seen that the bonding character of the 2-1' linkage was enhanced in HPBO and HPBI molecules but not at all in Tinuvin P. In Table VII, we show how the distance $r_{2-1'}$ is calculated to change with transfer of the OH proton. This distance remains unchanged for Tinuvin P (1.42 Å) and becomes shorter for the other two molecules HPBO and HPBI ($1.44 \to 1.41$ Å).

In simple words all these theoretical data indicate that in TIN a quinonoid form analogous to the one of HPBO and HPBI is

---

(95) Value extrapolated from 77 to 330 K by using the data of Figure 6 cited in ref 68 and ϕ_F (in 3MP) = 0.00020 from ref 5. We assumed that fluorescence quantum yields were extrapolable from glasses of 3MP to monocrystals since in HPBO ϕ_F^{77K}(crystals) = 0.42³ and ϕ_F^{140K} (inert solvents) = 0.395.[32]

(96) Catalan, J.; Perez, P. *J. Theor. Biol.* 1979, *81*, 213.

Table VII. Selected Calculated Geometrical Parameters for Tinuvin P, HPBI, and HPBO

	$r_{2-1'}$ (A)		
r_{O-H} (A)	R = Me X = Y = N Tinuvin P	R = H Y = NH; X = C HPBI	R = H Y = O; X = C HPBO
1.00	1.417	1.445	1.441
1.05	1.417	1.444	1.440
1.10	1.417	1.443	1.438
1.15	1.418	1.441	1.436
1.20	1.418	1.438	1.433
1.25	1.419	1.435	1.429
1.30	1.418	1.432	1.424
1.35	1.418	1.427	1.419
1.40	1.417	1.423	1.414
1.45	1.416	1.419	1.408
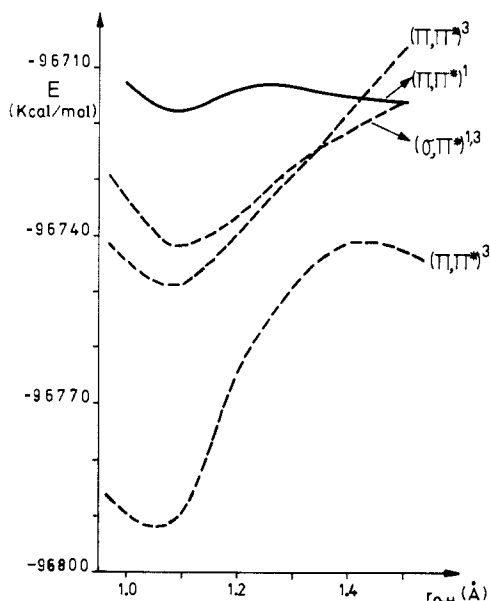
Figure 10. Proton-transfer Franck–Condon curves for several excited electronic states of TIN.

not possible, and we could also easily visualize it from the following chemical structures:

Y = O , HPBO
Y = NH, HPBI

TIN
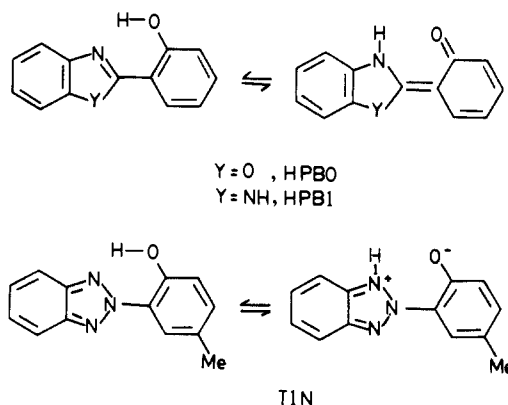
In Figure 10 we present the Franck–Condon curves corresponding to the proton transfer for several electronic states of Tinuvin P; it appears that there are the following: A T_1 triplet state strongly stabilized with respect to the excited singlet state. A T_2 triplet state of very short half-life that could probably be
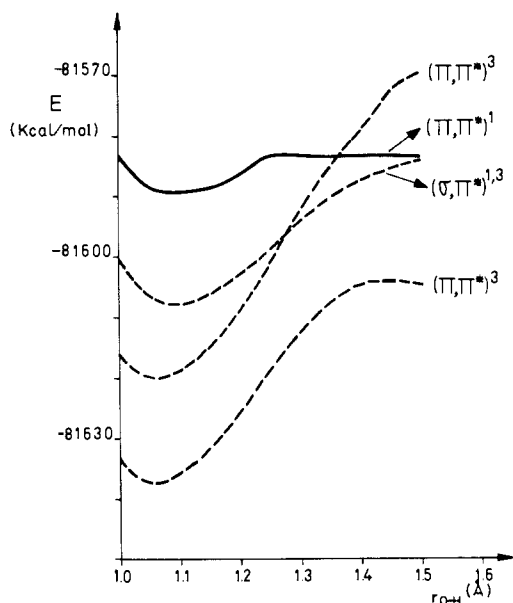

Figure 11. Proton-transfer Franck–Condon curves for several excited electronic states of 2-(pyrazol-1'-yl)-1,4-dihydroxybenzene (3).

Table VIII. CNDO/S Calculations Using Experimental X-ray Geometries for 2,3-Bis(pyrazol-1'-yl)-1,4-dihydroxybenzene (2)

state	λ (nm)	f	μ* (D)
1S	288.7	0.02	2.03
2S	242.7	0.04	4.11
3S	240.9	0.00	1.05
4S	236.7	0.00	5.23
1T	455.2		0.53
2T	452.3		5.68

Table IX. CNDO/S//INDO CI Calculations (with Mataga-Type Integrals) for 2-(Pyrazol-1'-yl)-1,4-dihydroxybenzene (3)

state	λ (nm)	f	α (deg)	μ* (D)
1(n,π*)¹	304.6			1.23
1(π,π*)¹	299.0	0.11	12.10	6.07
2(π,π*)¹	269.0	0.08	0.47	1.71
3(π,π*)¹	232.0	0.02	62.57	2.36
1(π,π*)³	493.4			1.87
2(π,π*)³	457.9			4.86

Table X. CNDO/S//INDO CI Calculations (with Mataga-Type Integrals) for 2,5-Bis(pyrazol-1'-yl)-1,4-dihydroxybenzene (4)

state	λ (nm)	f	α (deg)	μ* (D)
1(π,π*)¹	323.4	0.23	7.31	0.19
1(n,π*)¹	293.8			0.10
2(n,π*)¹	291.6			0.39
2(π,π*)¹	282.9	0.12	0.03	0.10
1(π,π*)³	500.9			0.67
2(π,π*)³	467.7			0.54

the triplet of energy 60 ± 1 kcal/mol previously detected by Werner. This T_2 triplet is not associated with proton transfer.

In summary, our photophysical data for Tinuvin P lead us to conclude that its ability to act as a UV stabilizer cannot be due to the formation of a transient quinonoid species in the 1(π,π*)¹ state by means of an ESIPT mechanism.

Theoretical and Photophysical Studies of 1-(2'-Hydroxy-phenyl)pyrazoles 1–4. A knowledge of the properties of these compounds will also help to answer the following questions. Will the presence of a second pyridine-like nitrogen atom in TIN, be a decisive factor in its nonfluorescence? How crucial is the rotation facility of the phenol group around the 2-1' bond in the 1(π,π*)¹ state for the photostability of that class of compounds? Is the presence of a triplet at a wavelength higher than 800 nm important for the observed decay of these UV stabilizers?
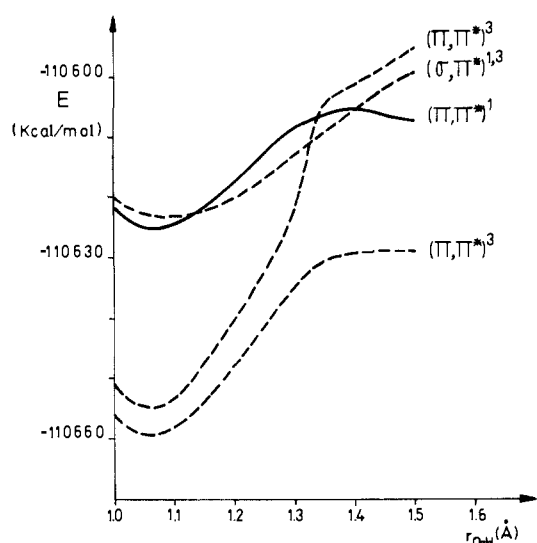
Figure 12. Single-proton-transfer Franck–Condon curves for several excited electronic states of 2,5-bis(pyrazol-1′-yl)-1,4-dihydroxybenzene (4).
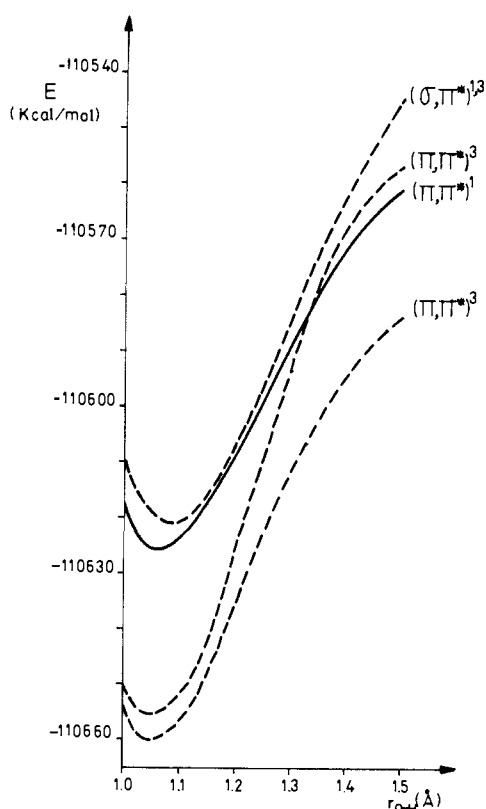

Figure 13. Double-proton-transfer Franck–Condon curves for several excited electronic states of 2,5-bis(pyrazol-1′-yl)-1,4-dihydroxybenzene (4).

We present in Figures 11, 12, and 13 the Franck–Condon curves corresponding to the proton transfer from the phenol oxygen to the pyrazole N-2 atom for several electronic states of the mono-pyrazolyl 3 and bis pyrazolyl derivative 4. From these theoretical results the following can be deduced. (1) Compounds 3 and 4 are unlikely to undergo an ESIPT process when irradiated. (2) The double proton transfer in derivative 4 is more difficult than a single proton transfer in the derivative 3 (compare Figures 11 and 13). (3) In derivative 3, as for TIN, the theoretical data of Figure 11 indicate the existence of a first singlet state (n,π^*) but not for the bis derivative 4. (4) For each of these compounds, there are two triplets $(\pi,\pi^*)^3$ which are energetically lower than the first singlet $(\pi,\pi^*)^1$. Contrary to what was predicted for Tinuvin P, the energies of the two triplets are similar, meaning

Table XI. UV Absorption Maxima of Derivatives 1–4

	λ_{max} (nm)			
compd	CyH (log ϵ)	ACN	DMSO	EtOH
1	317.0 (3.77)	305.5	307.3	306.2
2	320.7 (3.78)	313.1	311.1	311.0
3	318.3 (3.64)	314.9	312.7	311.6
4	341.2 (4.20)	335.4	326.5	328.0

Table XII. Emission Spectra of Derivatives 1–4 in CyH-EtOH[a] at 77 K

compd	concn (g/1.10³)	λ_{max}^{EM} [b] (nm)	τp (s)
1	7.2	425	0.26–0.38[c]
2	7.1	440	0.43
3	11.1	440	0.24
4	7.0	450	0.52

[a] The EtOH concentration is 2.5×10^{-1} M. [b] The used excitation wavelength corresponds to the absorption λ_{max} (see Table XI). [c] Observed variation range of a freshly prepared solution on standing.

Table XIII. Fluorescence Quantum Yields for Derivatives 1–4 at a λ^{EX} (nm) = 320

compd	ACN	DMSO	EtOH
1	0.006	0.093	0.066
2	0.002	0.101	0.052
3	0.008	0.158	0.058
4	0.003	0.327	0.102

no extra stabilization for any of them. (5) In the $1(\pi,\pi^*)^1$ state, these substances lose planarity by rotation around the pyrazole nitrogen-phenolic ring 2-1′ linkage. This conclusion, which can be explained by the nonbonding character of the π^* orbital, is in good agreement with the observed lack of fine structure of the first UV band.

In Tables VIII, IX, and X are gathered the calculated UV transitions for compounds 2, 3, and 4. All compounds exhibit a triplet $1(\pi,\pi^*)^3$ around 500 nm. Only derivative 4 shows a singlet $1(\pi,\pi^*)^1$ nature, and, therefore, a strong fluorescence is predicted for this derivative, as found by us and shown in Figure 14.

The electronic spectroscopy of these compounds has been studied in (i) nonpolar solvents that do not form hydrogen bonds, such as cyclohexane (CyH), (ii) polar aprotic solvents able to form slight hydrogen bonds, such as acetonitrile (ACN), or strong hydrogen bonds, such as dimethyl sulfoxide (DMSO), and (iii) polar protic solvents able to form hydrogen bonds, such as ethanol (EtOH).

In Table XI are given the absorption maxima of compounds 1–4 in CyH, ACN, DMSO, and EtOH. From these data it appears that derivatives 1, 2, and 3 have similar absorptions but that derivative 4 exhibits a max at longer wavelength with a much larger extinction coefficient.

Concerning emission spectra, the four compounds were neither fluorescent nor phosphorescent in CyH at room temperature or even at 77 K. When a small amount of EtOH is added to the foregoing solutions, they become fluorescent with maxima at 350–365 nm at room temperature and strongly phosphorescent with maxima around 440 nm at 77 K (see Table XII).

Also in order to estimate the intensity of these phosphorescences, we have determined the quantum yields at 77 K and EPA as the solvent for 2,5-bis(pyrazol-1′-yl)-1,4-dihydroxybenzene (4) λ^{EX} (nm) = 335; λ^{EM} (nm) = 450; ϕ_p = 0.922; τ_p (s) = 0.52; and Tinuvin P λ^{EX} (nm) = 300; λ^{EM} (nm) = 445; ϕ_p = 0.986; τ_p (s) = 0.43. The literature[51] reported values for Tinuvin P are ϕ_p = 0.985 and τ_p (s) = 0.415.

The fluorescence spectra at room temperature of compounds 1–4 in ACN, DMSO, and EtOH air-equilibrated solutions are shown in Figure 14; Table XIII reflects the respective quantum yields.

Photostability Studies. Preliminary experiments on the determination of photolysis quantum yields of compounds 1–4 in CyH solutions showed they have a high stability. Their insolubility in CyH prevented us from obtaining acceptable absorptions.
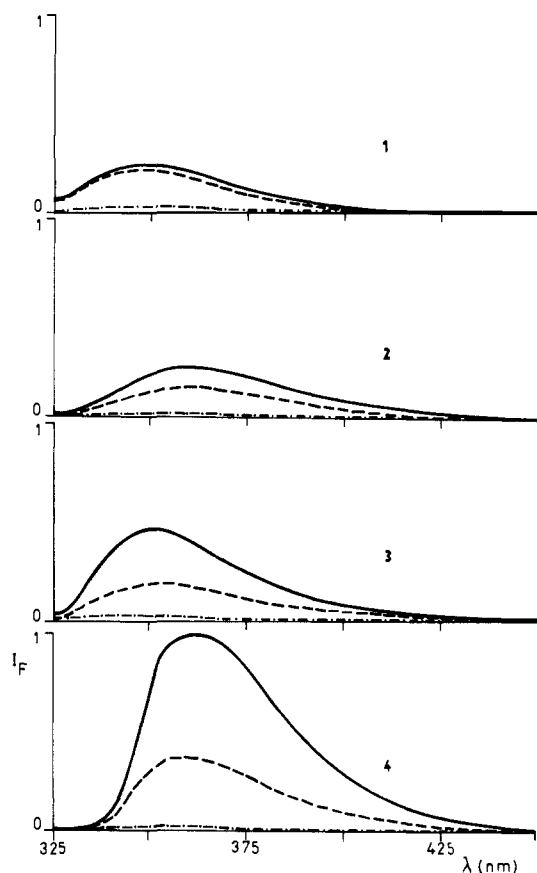
Figure 14. Fluorescence spectra of compounds 1–4 in acetonitrile (ACN, ·–·), dimethyl sulfoxide (DMSO, —), and ethanol (EtOH, --).

Therefore we carried out a comparative study of their photostability with the "UV-accelerometer system".[83]

CyH solutions of compounds 1–4 and Tinuvin P of normalized absorbance at temperature 40 ± 1 °C were irradiated simultaneously. The degradative processes were followed spectrophotometrically, and in all cases a diminution of the original absorption maxima with formation of an isosbestic point at ∼340 nm was observed. For very long irradiation periods an absorption toward 350–380 nm also appeared.

From the slope of the linear relationship of absorbances (Abs_t/Abs_0) in CyH against irradiation time (see Figure 15) for compounds 2, 4, and Tinuvin P a quantitative estimation of their photostability is obtained. Thus, the photodegradability order after 1 h of irradiation is

$$2(5 \times 10^{-3}) > 1(3.67 \times 10^{-3}) > 3(2.67 \times 10^{-3}) >$$
$$4(2 \times 10^{-3}) > TIN(0.67 \times 10^{-3})$$

For longer irradiation periods, the linearity disappeared, and a progressive diminution of the slope value occurred. This was due to the lowering of absorbed intensity on diminution of the initial concentration of the samples.

To check of the presence of an IMHB was the reason for the stability differences of products 1–4 in CyH solutions, the experiments were repeated for the derivatives 2 and 4 but with the addition of an extra amount of EtOH (2.5 × 10⁻¹ M) in order to form intermolecular hydrogen bonds. The presence of EtOH did not affect the stability of 2,3-bis(pyrazol-1'-yl)-1,4-dihydroxybenzene (2) but clearly diminished that of 2,5-bis(pyrazol-1'-yl)-1,4-dihydroxybenzene (4). This behaviour seems to be due to the fact that compound 4 has a much stronger IMHB in cyclohexane than does the 2 derivative; this intramolecular hy-
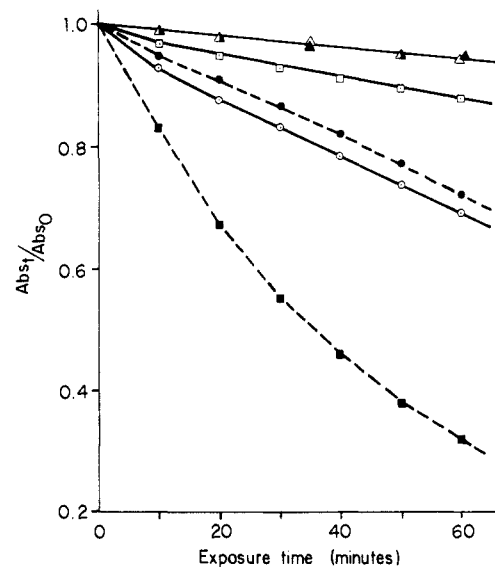

Figure 15. Changes in absorbance as a function of ultraviolet exposure for solutions of the following: Tinuvin P in (▲) pure cyclohexane and (△) cyclohexane containing ethanol (2.57 × 10⁻¹ M); 4 in (□) pure cyclohexane and (■) cyclohexane containing ethanol (2.57 × 10⁻¹ M); and 2 in (○) pure cyclohexane and (●) cyclohexane containing ethanol (2.57 × 10⁻¹ M).

drogen bond is disrupted by the presence of ethanol.

In order to know the actual properties of these new pyrazole derivatives we have added them to polystyrene, and the study of photoprotection effects is now in progress with very promising preliminary results.

Conclusions

The following four new compounds 1,4-dihydroxy-2,3-bis-(3',5'-dimethylpyrazol-1'-yl)benzene (1) and 1,4-dihydroxy-2,3-bis(pyrazol-1'-yl)benzene (2) (both nonplanar derivatives) and 1,4-dihydroxy-2-(pyrazol-1'-yl)benzene (3) and 1,4-dihydroxy-2,5-bis(pyrazol-1'-yl)benzene (4) (both planar derivatives), which are structurally related to 2-(2'-hydroxy-5'-methylphenyl)-benzotriazole (Tinuvin P), exhibit excellent stability to light.

Experimental evidence in this paper proves the existence of a triplet beyond 800 nm with a short half-life which is not associated with proton transfer in Tinuvin P. Theoretical calculations show that quinonoid forms in Tinuvin P and in derivatives 1–4 are not favored. Thus, we can conclude that the photophysical behavior of all these compounds is not a consequence of an excited state intramolecular proton transfer (ESIPT) as in 2-hydroxybenzophenones or methyl salicylates.